Journal of Bio- and Tribo-Corrosion (2020) 6:135
https://doi.org/10.1007/s40735-020-00432-0

A Review on Bio-functionalization of β-Ti Alloys

I. Çaha[1] · A. C. Alves[1] · L. A. Rocha[2,3] · F. Toptan[1,4]

Received: 17 August 2020 / Revised: 17 September 2020 / Accepted: 29 September 2020 / Published online: 10 October 2020

Abstract
β-Ti alloys are known for their very low Young's modulus, excellent physical properties, and biocompatibility, hence they are considered as attractive metallic materials for long-term bone implant applications. However, β-Ti alloys are poor wear resistant and typically bioinert materials, thus their surfaces need to be modified to have wear resistant and bioactive properties. In this paper, an overview is given to the available surface functionalization techniques to improve the biological properties of β-Ti alloys. Mechanical, physical, chemical, and electrochemical treatments, as well the immobilization of bio-functional molecules are discussed. Bioactivity, biocompatibility, haemocompatibility, wear and/or corrosion, behaviour of the β-Ti alloys can be improved using a proper surface modification technique, by altering the surface composition and topography or removing the undesired material from the alloy surface.

Keywords β type titanium alloys · Surface modifications · Bio-functionalization · Biomedical implants

1 Introduction

Several biomaterials are available for being used as implant materials, such as metals (stainless steel, Co-based alloys, Ti and its alloys), ceramics (alumina, zirconia, calcium phosphates), and synthetic or natural polymers [1]. In the last few decades, metallic biomaterials have been extensively used in biomedical applications mainly due to their excellent mechanical properties [2]. Among those, Ti and its alloys are considered as the most suitable biomaterials owing to their high strength, excellent corrosion resistance, and biocompatibility [3–5].

Ti alloys are classified as α, β, near-α, α + β, and metastable β phases [6]. In this context, the alloying elements are grouped into three categories: α-stabilizers such as Al, O, N, C, β-stabilizers such as Mo, V, Fe, Cr, Ni, Co, Nb, Ta, Mn, and neutrals such as Sn and Zr [5]. The α and near-α Ti alloys have good fracture toughness and corrosion resistance but have limited mechanical strength. On the other hand, the α + β Ti alloys exhibit higher strength, higher ductility, and higher low-cycles fatigue strength [5]. α + β type Ti–6Al–4V alloy (ASTM F1108) is the most popular Ti alloy and has been used for producing orthopaedic prostheses and dental implants due to its excellent specific strength, corrosion resistance, and biocompatibility [7]. However, ions of the alloying elements have been linked with various health problems such as neurological diseases and cytotoxic effects of Al and V, respectively [8–13].

Widely used α-type and α + β-type Ti-based implant materials have Young's modulus values around 100–120 GPa, whereas Young's modulus of bone is 5–6 times lower than those materials [14–16]. The Young's modulus of human cortical bone is about 15–20 GPa, more specifically, the Young's modulus of the fibula is about 15–20 GPa, the humerus is about 15–16 GPa, the tibia is about 16–19 GPa and the femur is about 13–15 GPa [17]. The difference in Young's modulus between implant and bone causes the unbalanced distribution of stress on bone leading to bone resorption. Therefore, it causes poor osteointegration which may subsequently lead to loosening or failure of the implant [18–20]. This mechanism, that is known as stress-shielding

✉ I. Çaha
ihsancaha@gmail.com

1 CMEMS-UMinho – Center for MicroElectroMechanical Systems, Universidade do Minho, Azurém, 4800-058 Guimarães, Portugal

2 Tribocorrosion and Nanomedicine, IBTN/Br – Brazilian Branch of the Institute of Biomaterials, Bauru, SP, Brazil

3 Dep. Física, Faculdade de Ciências de Bauru, UNESP—Univ. Estadual Paulista, Bauru, SP 17033-360, Brazil

4 IBTN/Euro – European Branch of the Institute of Biomaterials, Tribocorrosion and Nanomedicine, Dept. Eng. Mecânica, Universidade do Minho, Azurém, 4800-058 Guimarães, Portugal

and it can be minimized using an implant material having Young's modulus closer to the bone.

Ti alloys with low Young's modulus have been developed using biocompatible, non-toxic β-stabilizers elements such as Nb, Zr, Ta, Mo [4, 14, 21–29]. Niinomi et al. [3] and Abdel-Hady et al. [30] reported that Young's modulus can be significantly reduced by adjusting the concentration of β-stabilizing elements. As reported by previous studies [31, 32], the β-type Ti alloys especially with Nb contents have been received attention and investigated extensively because of non-toxicity, good biocompatibility, also, better cell adhesion, proliferation, and differentiation in vitro. During the last two decades, many novel non-toxic and allergy-free β-Ti alloys have been produced with displaying superior corrosion resistance and good biocompatibility along with their low Young's modulus [33–35]. Some of β-Ti alloys, such as Ti–29Nb–13Ta–4.6Zr, include high cost, non-toxic and allergy-free elements such as Nb, Ta, Zr and Mo [36]. Thus, instead of these rare and expensive elements, low-cost elements such as Fe, Cr, Mn, and Sn are also used to produce low Young's modulus β-Ti alloys, like Ti–Mn–Fe [37] or Ti–Sn–Cr [38]. The load-bearing implant materials are expected to exhibit a combination of high strength and low Young's modulus [39], however, the lowest Young's modulus β-Ti alloys also have poor yield and tensile strength because, in general, these alloys are produced under solutionized conditions [40]. Therefore, the strength of β-Ti alloys needs to be increased while keeping their Young's modulus, in order to improve the performance of the implants. Some available techniques to increase the strength are cold working [41], accumulative roll bonding [42], aging treatment, spark plasma sintering (SPS), and plastic deformation (especially high-pressure torsion) [43–47]. Datta et al. [48] used a predictive model and showed that increased content of β-stabilizers could reduce the strength of the β-Ti alloys. The incorporation of some β-stabilizers may also increase the strength of the alloys, as in the case of Ti6Al4V that presents higher strength as compared to cp-Ti. Also, the incorporation of Ta to Ti–Nb–Zr increase tensile strength and decrease Young's modulus [28]. Nevertheless, the incorporation of elements does not always improve the mechanical properties of β-Ti alloys like in the case of incorporation of Sn to Ti–Nb which drastically decreases the tensile strength [39]. On the other hand, solid solution strengthening by oxygen is also effective in improving the strength of β-Ti alloys as maintaining their low Young's modulus [49]. Niinomi and Nakai [50] reported that a small content of oxygen resulted in an increase in the strength, however, it also led to an increase in Young's modulus for Ti–29Nb–13Ta–4.6Zr alloy.

Surface degradation of implants is one of the most important drawbacks for long-term implantation in the human body. When a metallic implant inserted into the human body, it can release metallic ions due to corrosive conditions [51]. Ti presents superior corrosion behaviour due to the spontaneously formation of a very stable oxide layer (passive film) on its surface. This passive film protects the implant materials against corrosion, reduces the release of metallic ions, and it is responsible for good biocompatibility. However, the corrosion behaviour of β-Ti alloys is determined by the role of β-stabilizing elements on the passive film.

Ti–Nb alloys have a great interest because of good biocompatibility and corrosion behaviour. Ti–Nb has better corrosion behaviour than cp-Ti [52, 53] and Ti–Mo [54]. Moreover, minor incorporation of Ru [55], In [56], and Sn [57] is reported to improve the corrosion behaviour. However, the commercial Ti–6Al–4V alloy presented better corrosion resistance than Ti–40Nb alloy through an immersion period of 21 days in NaCl solution that attributed to the formation of a more stable and thicker passive film [58]. The contribution of Zr, Ta, Mo, etc. β stabilizers in Ti–Nb alloys improved their corrosion behaviour in different physiological solution through the formation of a mixed passive oxide layer that had been reported to be more stable [59–67]. Ti–Mo, Ti–Zr, and Ti–Ta based β-Ti alloys are also popular alloys thanks to their unique properties such as non-toxicity, good mechanical properties, and relatively better corrosion resistance [68, 69]. Binary Ti–Mo [70–72], Ti–Zr [73–75], and Ti–Ta [76–78] alloys presented better corrosion resistance than cp-Ti in different solutions, while the ternary and multinary of these alloys exhibited further improvement in their corrosion behaviour [79–82].

Tribocorrosion is defined as an irreversible degradation process on the material surfaces subjected to the combined action of wear and corrosion [83]. Ti alloys are shown to possess poor wear resistance being a limiting factor in many applications [84, 85]. Although it is known that the total degradation rate after tribocorrosion can be different than the sum of the individual corrosion and wear rates, the literature reporting the synergistic interactions between corrosion and wear on β-Ti alloys is still scarce. Cvijović-Alagić et al. [86] investigated the tribocorrosion behaviour of Ti–13Nb–13Zr alloy in comparison with Ti–6Al–4V in Ringer's solution and found that Ti–13Nb–13Zr alloy had a substantially lower wear resistance than Ti–6Al–4V alloy. Similar behaviour was reported for Ti–40Nb alloy tested in 9 g/L NaCl solution [58]. On the other hand, Correa et al. [87] compared the tribocorrosion behaviour of Ti–15Zr–7.5Mo and Ti–15Zr–15Mo β-Ti alloys and reported a better behaviour for the Ti–15Zr–7.5Mo alloy. More et al. [88] studied the tribocorrosion behaviour of Ti–12.5Mo, Ti–13Nb–13Zr and Ti–29Nb–13Ta–4.6Zr β-Ti alloys and Ti–6Al–4Fe α + β-Ti alloy against polyethylene in Hank's balanced salt solution. The authors reported that the β-Ti alloys induced lower wear damage on the counter material. Besides, the addition of synovial fluid constituents (bovine serum albumin,

hyaluronic acid, and dipalmitoylphosphatidylcholine) increased the wear volume loss on the Ti–29Nb–13Ta–4.6Zr alloy. Pina et al. [89] studied the influence of Sn addition on the tribocorrosion behaviour of Ti–Nb based β alloy and reported that Sn addition resulted with an increased wear volume loss in phosphate-buffered solution (PBS).

In order to improve the integration of bone and tissue, several surface modification techniques have been used to tailor the topography [21, 90–95]. When the properties of the implant surface can mimic the physical and chemical properties of the biological structure, tissue and implant surface integration is accomplished by adhesion, spreading and proliferation of cells on the implant surface [96]. On the other hand, coatings improve the surface properties including the hardness, wettability, elastic strain, coefficient of friction, and wear resistance. Coating materials used in joints replacement are fabricated by physical and chemical vapor deposition (PVD and CVD, respectively), electrodeposition, and ion implantation [97–101]. On the other hand, owing to their unique wear and tribocorrosion properties, metal matrix composites (MMCs) can be considered for orthopaedic and dental implants as a coating material or as a functionally graded material (FGM) [102–109]. Besides, nanostructured surfaces have also been studied to achieve better adhesion between the biomedical application and tissue [110–115].

β-Ti alloys considered as promising metallic materials for long-term bone implant applications. However, these alloys have some limitations such as poor wear resistance, still higher Young's modulus compared to that of the bone, and lack of bioactivity. Therefore, a focus is given on both producing new β-Ti alloys, and improving their mechanical, tribological, electrochemical, triboelectrochemical, and biological properties. So, the studies on β-Ti alloys, particularly bio-functionalization studies are very important for the future improvements. Hence, this review aimed at gathering and summarizing the available state-of-art techniques to bio-functionalize the β-Ti alloys to obtain multifunctional implants.

2 Bio-functionalization of β-Ti Alloys

Metallic biomaterials have an attractive combination of high durability, high toughness, non-toxicity, and high strength. However, metallic biomaterials are typically artificial materials, therefore, their surfaces need modification to gain bioactive properties. The biomaterial surface plays an extremely significant role when interfacing with the biological environment (neutral tissue). Ti-based implants usually manufactured by melting, casting, forging, heat treatment, and oxidation which usually lead to a contaminated surface layer that is often stressed and plastically deformed, and non-uniform. Such native surfaces are not suitable for biomedical applications and some surface treatments should be performed. At the same time, different bio-functions are required depending on the intended implant location to achieve biological integration. For example, blood compatibility (haemocompatibility) is very important for blood-contacting biomedical devices such as stent and catheter, whereas osteointegration is a crucial parameter for bone applications. When a metallic biomaterial is implanted into a blood-contacting location, the first rapid event takes place is the blood protein adsorption leading to structural alterations that allow biological interactions. Thus, over time, a built-in protein layer is formed that affects the interaction of platelets, the adhesion, and aggregation of platelets. Concerning bone applications (orthopaedics and dentistry), once the implantation procedure occurs, the implant surface is wetted and the biologically active molecules (such as proteins) are adsorbed quickly followed by the osteoprogenitor cells that would regenerate the tissue [116]. The two main factors affecting osteointegration are the mechanical properties of the implant and the biological interactions with the metal surface, being the second the most relevant. Another important reason for the surface modification is to increase the corrosion and wear resistance of the metallic biomaterial. As a result, bioactivity, biocompatibility, haemocompatibility, wear, and corrosion resistance of the metallic biomaterials can be improved by surface modification, altering the surface chemical composition, topography, and crystal structure or removing the undesired material from the metallic biomaterial surface. For this purpose, many techniques have been applied for the surface modification of metals, some of which have also been commercialized.

It is clear that a biomaterial response is dependent on its biocompatibility and surface properties. In the literature, the bio-functionalization of metallic biomaterials, especially Ti and Ti6Al4V has been extensively studied and it is still being researched as recently reviewed by Su et al. [117]. Despite the combination of their unique features, β-Ti alloys need to be bio-functionalized to increase tissue adhesion and implant integration, to decrease bacterial adhesion, and inflammatory response or to avoid the foreign body response. In the following sections, the surface modifications that are investigated for β-Ti alloys are discussed. These treatments are being applied individually or as a combination.

2.1 Mechanical Treatments

The biomechanical properties and bioactivity of the implant surface can be improved by mechanical treatments, overviewed in Table 1, yielding with the nanostructured and ultrafine-grained surface with enhanced strength. Electric discharge machining (EDM) has been widely studied on cp-Ti and Ti–6Al–4V alloy to improve their hardness,

Table 1 Overview of mechanical treatments applied for β-Ti alloys

Methods	Objectives	Alloys applied
Powder mixed electric discharge machining (PMEDM)	Fabricating a 3–18 μm nanoporous recast layer	Ti–35Nb–7Ta–5Zr [119–123]
Surface mechanical attrition treatment (SMAT)	Producing rough and hard a gradient nanostructured material	Ti–30Nb–8Zr–0.8Fe [127] Ti–34Nb–2Ta–0.5O [128] Ti–25Nb–3Mo–3Zr–2Sn [129] Ti–5Al–2Sn–2Zr–4Mo–4Cr [130] Ti–25Nb–3Mo–2Sn–3Zr [131] Ti–32Nb–2Sn [296]
Ultrasonic nanocrystal surface modification (UNSM)	Inducing severe plastic deformation at the surface to generate a gradient nanostructured surface	Ti–29Nb–13Ta–4.6Zr [133, 134, 297]
High-pressure torsion (HPT)	Obtaining ultrafine-grained metallic materials to increase the mechanical strength and decrease or retain Young's modulus	Ti–29Nb–13Ta–4.6Zr [43, 44, 137, 140] Ti–13Nb–13Zr [141, 145] Ti–24Nb–4Zr–8Sn [142, 298] Ti–45Nb [139] Ti–15Mo [143, 299] Ti–20Mo [136] Ti–24.6Nb–5Zr–3Sn [135] Ti–19.6Nb–4.5Ta–2.4Cr [135] Ti–19Nb–7Mo–14Zr [300] Ti–28Nb–8Mo–12Zr [300] Ti–35Nb–7Zr–5Ta [144]
Accumulative roll bonding (ARB)	Production of metallic materials with ultrafine grained microstructure to improve mechanical properties	Ti–10Zr–5Nb–5Ta [147, 148] Ti–25Nb–25Ta [146, 149] Ti–25Nb–3Zr–3Mo–2Sn [150, 151]

corrosion and wear properties [118]. In the case of β-Ti alloys, the Ti–35Nb–7Ta–5Zr alloy has been studied by powder mixed electrical discharge machining (PMEDM). A schematic diagram of the PMEDM process and examples for the resulting microstructures on Ti–35Nb–7Ta–5Zr alloy is given in Fig. 1. PMEDM treated alloy presented better hardness, corrosion resistance, cell adhesion, cell spreading, and cell differentiation compared to the unmachined one, attributed to the formation of a nanoporous recast layer [119–123].

The surface mechanical attrition treatment (SMAT) is a method that can be used to tailor the mechanical and tribological properties of a surface [124, 125]. The SMAT device mainly consists of a vibration generator and a treatment chamber having balls as shown in Fig. 2a. The SMAT treatment was reported to improve the corrosion resistance, fatigue resistance, osteointegration, and haemocompatibility due to nanocrystallization of the cp-Ti surface [126]. Regarding β-Ti alloys, SMAT treated Ti–30Nb–8Zr–0.8Fe alloy having β grains around 150 μm (Fig. 2b) modified to a nanocrystalline structure having grains of several tens of nanometres (Fig. 2c) that led to an increase on the surface hardness [127]. The increased hardness of the surface decreased the wear rate of materials, such as the reduction of the fretting wear rate of Ti–34Nb–2Ta–0.5O alloy immersed in a 20% foetal bovine serum solution (pH 7.4) [128]. The corrosion behaviour of Ti–25Nb–3Mo–3Zr–2Sn and Ti–34Nb–2Ta–0.5O alloys in SBF solution was

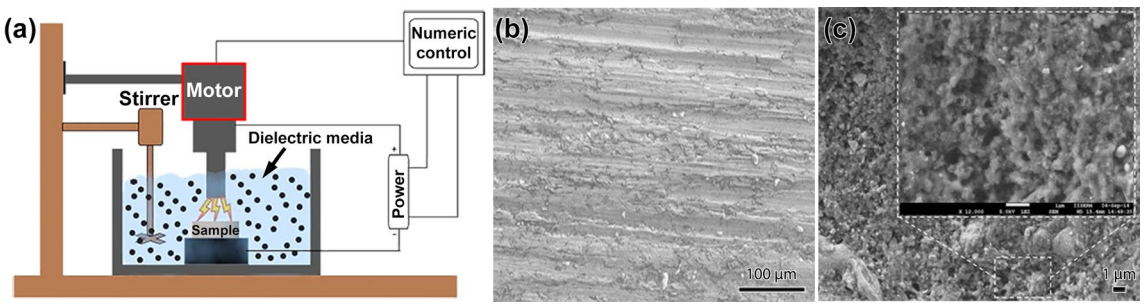

Fig. 1 **a** Schematic diagram of PMEDM process and examples for the resulting microstructures on Ti–35Nb–7Ta–5Zr alloy **b** before and **c** after treatment (adapted from [119] with permission from Springer)

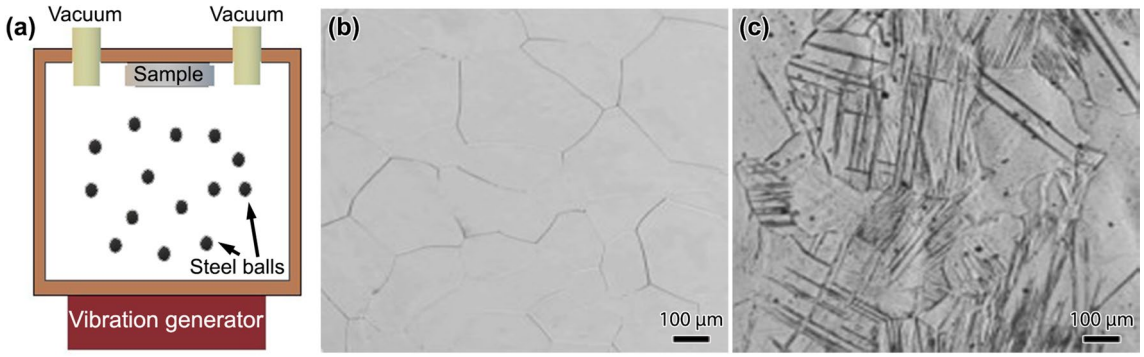

Fig. 2 **a** Schematic diagram of SMAT process and representative microstructures on Ti–30Nb–8Zr–0.8Fe alloy **b** before and **c** after treatment (microstructure of alloy was taken from [127] with permission from Elsevier)

improved after SMAT treatment associated with the formation of a denser passive oxide layer resulted from the grain refinement [128, 129]. However, corrosion resistance of Ti–5Al–2Sn–2Zr–4Mo–4Cr alloy in 3.5% NaCl solution was decreased after SMAT treatment due to residual internal stress created from the treatment process [130]. The authors reported that stress relief heat treatment of 250–350 °C can significantly improve the corrosion resistance of SMAT treated alloy. In vitro cell culture studies indicated a significant improvement in cell adhesion, proliferation, differentiation, extracellular matrix mineralization, and protein absorption of SMAT treated Ti–25Nb–3Mo–2Sn–3Zr alloy as compared to the non-treated alloy due to its superior hydrophilicity, nanostructured surface, and increased surface roughness [131].

Ultrasonic nanocrystal surface modification (UNSM) is a novel method to induce severe plastic deformation at the surface to generate a gradient nanostructured surface layer on metallic materials. The process uses super-encapsulated ultrasonic vibration on the combination of static and dynamic loads to create high-strain rate plastic deformation on a material surface (Fig. 3a) [132]. Kheradmandfard et al. [133] applied the UNSM process to a Ti–29Nb–13Ta–4.6Zr alloy and obtained a significant increase on the surface hardness (≈ 385 HV) as compared to the untreated alloy (190 HV) owing to the surface structure having nanoscale lamellae and nanostructured subgrains (Fig. 3b), along with high dislocation density and α precipitates. The authors also reported that UNSM treated Ti–29Nb–13Ta–4.6Zr alloy presented significantly better wear resistance, cell adhesion, spreading, and proliferation attributed to both nanoscale grain refinement and micro-patterned surface effects (Fig. 3c) [134].

High-pressure torsion (HPT) is another commonly used severe plastic deformation technique to obtain ultrafine-grained structure for improving mechanical properties, particularly hardness and ductility as well as its biofunctionality [44, 135–138]. A schematic diagram of HPT process is given in Fig. 4a together with the representative microstructures on Ti–45Nb alloy before (Fig. 4b) and after (Fig. 4c, d) HPT deformation with 5 GPa pressure and $n = 5$ rotation number, where the grain size was reported to be decreased from around 20 µm to less than 100 nm [139]. As expected, HPT treatment improved the mechanical and microstructural properties of different β-Ti alloys [139–144]. Regarding corrosion, HPT treated Ti–13Nb–13Zr alloy

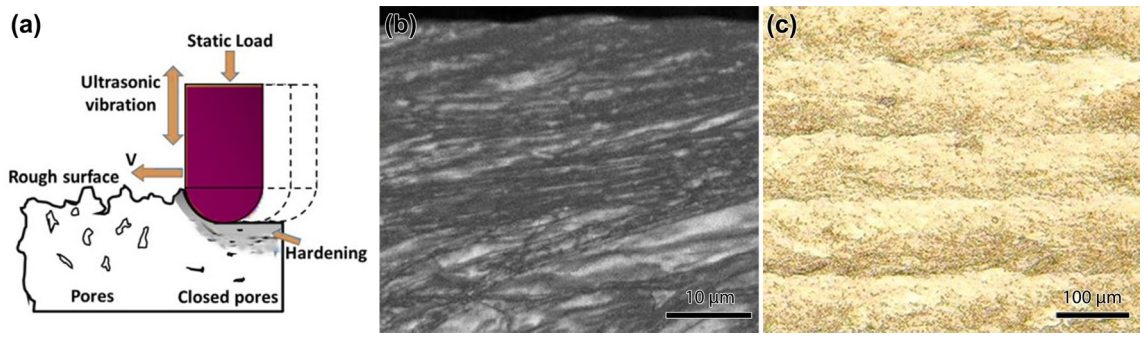

Fig. 3 **a** Schematic diagram of the UNSM process (adapted from [132]) and representative resultant surfaces on a Ti–29Nb–13Ta–4.6Zr alloy: **b** SEM image, **c** laser scanning microscope image (adapted from [133] with permission from Elsevier)

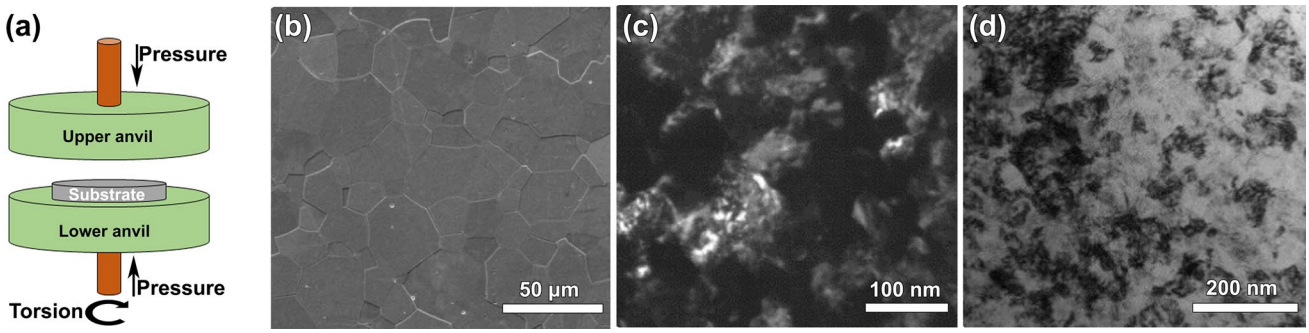

Fig. 4 **a** Schematic diagram of HPT process and representative microstructures: **b** optical microscope image of the initial Ti–45Nb alloy, **c** dark and **d** bright-field TEM images of the alloy after HPT treatment under 5 GPa pressure and 5 rotation number (adapted from [139] with permission from Elsevier)

showed significantly higher corrosion resistance in artificial saliva solution as compared to the untreated alloy associated with the grain size reduction to ultrafine range [140]. However, the quantities of released ions from HPT treated Ti–13Nb–13Zr alloy were higher than the quantities from untreated alloy, explained by its smaller grains, which was more prone to the release metallic ions [145]. In vitro cell culture tests revealed that the HPT treatment significantly increased the cell attachment, spreading, and proliferation on the treated samples influenced by their increased wettability due to their high internal energy given by the nano-sized grains having increased numbers of boundaries, interfaces, and dislocation density [140, 141]. Furthermore, alkaline treatment and the nanotubular layer formed on HPT treated β-Ti alloys presented better bioactivity as compared to the non-HPT treated one, explained by changing surface chemistry after chemical and anodic treatments [144].

Accumulative roll bonding (ARB) is another severe plastic deformation technique that has been applied to different β-Ti alloys to improve their functionality through grain refinement [146–151]. The studied β-Ti alloys presented better mechanical and corrosion behaviour as compared to the as-cast alloys due to the formation of nano-sized refined grains. However, biological studies are needed to understand the effect of ARB treatment on the bioactivity of β-Ti alloys.

2.2 Physical Surface Treatments

Physical surface treatments of β-Ti alloys including PVD, plasma spraying, plasma nitriding, gas nitriding, and ion implantation treatments are overviewed in Table 2 and demonstrated in Fig. 5 with the examples of surface and subsurface microstructural images. PVD processes are carried out in vacuum and the material are coated with positively charged ions during the process, resulting with a very strong bonding between the coating film and the substrate (Fig. 5c). The plasma spray process is the spraying of molten or thermally softened material to the surface to provide a coating [152]. On the other hand, ion implementation technique provides an easy control on the energy of ions, giving a good adhesion between the coating layer and the substrate resulted from gradient film coatings as shown in Fig. 5d, e. This technique allows to control the thickness of the coating, and eliminates the contamination since the process is carried out in vacuum [152].

Hydroxyapatite (HA, $Ca_{10}(PO_4)_6(OH)_2$) is a bio-ceramic material having a very similar chemical and crystallographic structure to human bone. HA has remarkably high biocompatibility thus it is used to improve the osteointegration process. However, its mechanical properties such as tensile strength and fracture toughness are quite poor, making it unsuitable for load-bearing implant applications. Various types of surface modification techniques have been used to deposit HA layers on Ti and its alloys, such as plasma spraying, sol–gel method, electrochemical deposition, and radio frequency (RF) sputtering. Zhao et al. [153] studied the microstructures, mechanical properties, and apatite-induction abilities of HA/Ti composite coating Ti–24Nb–4Zr–7.9Sn β-type alloy by plasma spraying. The authors reported that the microstructure, mechanical properties, and apatite-induction ability were influenced by the HA/Ti powders ratio used on processing. Also, the increase on Ti content led to an increase on the mechanical properties, however, decreased the apatite-induction ability. Zhao et al. [154] also studied the influence of the processing temperatures on Ti–24Nb–4Zr–7.9Sn alloy surface after plasma sprayed HA coating and reported that martensitic transformation and recrystallization influenced the mechanical properties resulting with a slight increase in the tensile and yield strengths but also led to a significant increase in Young's modulus (from 56.9 to 73.2 GPa). The main disadvantage of the plasma spraying technique is the poor adhesion between HA and the substrate materials. In order to improve the adhesion between HA and β-Ti alloys, some other techniques were also studied. He et al. [155] produced Ti–13Nb–13Zr–10HA composites by spark plasma sintering

Table 2 Overview of physical surface modification methods applied for biomedical β-Ti alloys

Methods	Objectives	Alloys
Plasma spray	Improving wear resistance, corrosion resistance and biological properties	Ti–24Nb–4Zr–7.9Sn [153, 154] Ti–13Nb–13Zr [158, 159]
Gas nitriding		Ti–27Nb [160, 167] Ti–16Mo [170] Ti–15Mo–5Zr–3Al [161] Ti–15Mo–3Nb–3Al–0.2Si [169]
Plasma nitriding		Ti–15Mo [163] Ti–13Nb–13Zr [164] Ti–15Mo–3Nb–3Al–0.2Si [162, 174]
PVD		Ti–12Mo–6Zr–5Sn–0.4Fe [166] Ti–13Nb–13Zr [294, 301, 302] Ti–45Nb [165] Ti–15Mo [163]
Sputtering		Ti–35Ta–*x*Zr (*x* = 3, 7, and 15) [157] Ti–13Nb–13Zr [164]
Ion implantation	Modifying surface composition; improving wear, corrosion resistance, and biocompatibility	Ti–25Ta–25Nb [173] Ti–35Nb–7Zr–5Ta [171] Ti–10Zr–10Nb–5Ta [172]
Plasma immersion ion implantation (PIII)		Ti–13Nb–13Zr [175] Ti–15Mo–3Nb–3Al–0.2Si [303]
Glow discharge plasma	Obtaining a clean, sterilize, oxide, nitride surface; removing the native oxide layer	Ti–5Zr–3Sn–5Mo–15Nb [304]

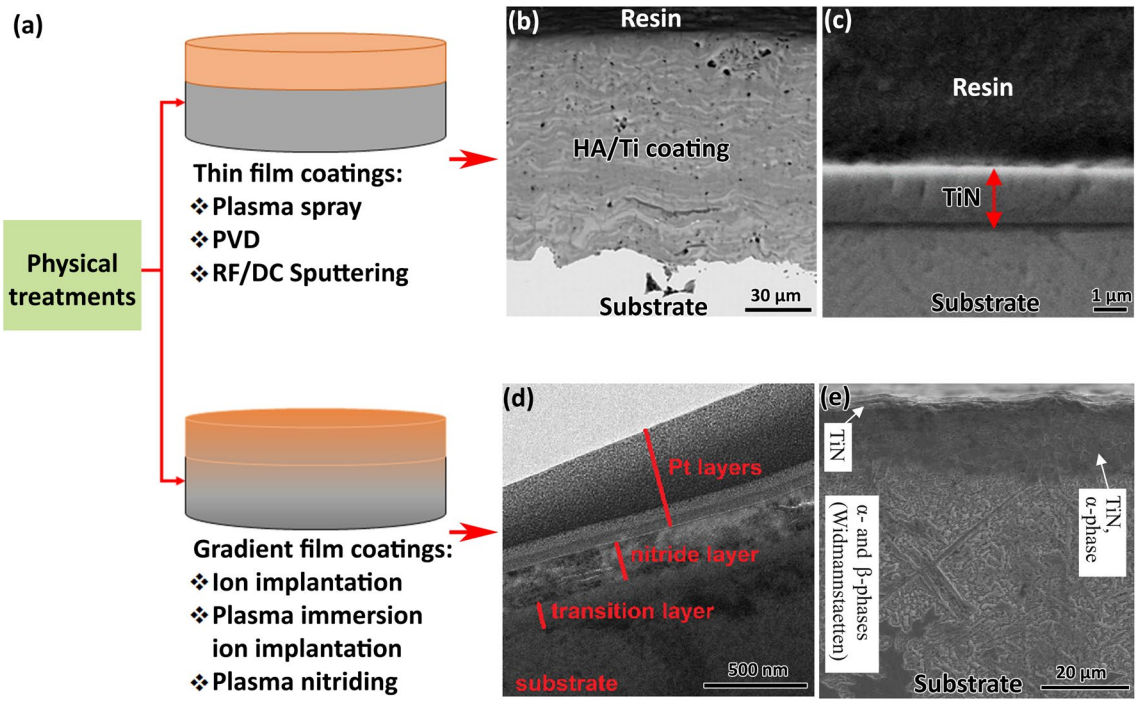

Fig. 5 **a** Schematic illustration of physical surface functionalization with resultant images: **b** cross-sectional SEM image of plasma sprayed HA/Ti coating on Ti–24Nb–4Zr–7.9Sn (adapted from [153] with permission from Elsevier), **c** cross-sectional SEM image of TiN coated on Ti–13Zr–13Nb alloy using cathodic arc physical vapor deposition (CAPVD) method (adapted from [294] with permission from MDPI, **d** TEM cross-section image of the nitrogen implanted Ti–35Nb–7Zr–5Ta alloy (adapted from [171] with permission from Elsevier), **e** cross-section SEM image of gas nitrided of Ti–15Mo–5Zr–3Al (adapted from [161] with permission from Elsevier)

process at sintering temperatures varying between 950 and 1150 °C. The authors reported that mechanical properties of the composite, namely compressive strength, yield strength, and hardness were increased with the increased processing temperature. However, the processing temperatures above 1050 °C led to an intense reaction between Ti and HA increased in the metal-ceramic reaction phases. Depending on the processing technique and processing temperature, the thermal decomposition of HA during the processing of Ti–HA composites may lead to a decrease in the corrosion resistance due to the formation of locally active sites on the HA-depleted zones [156]. However, if the decomposition of HA is not observed, Ti–HA composite surfaces may increase the corrosion resistance. For instance, Kim et al. [157] studied the surface characteristics of Ti–HA composite coatings developed on Ti–35Ta–*x*Zr alloy surfaces having 3, 7, and 15 wt% of Zr through RF and direct current (DC) sputtering and reported that the composite layer improved the corrosion resistance of the bare alloy by forming a stable barrier against corrosion.

The Al_2O_3–$13TiO_2$, ZrO_2 and the bilayered (ZrO_2/Al_2O_3–$13TiO_2$) nanoceramics coated by plasma spray technique on Ti–13Nb–13Zr alloy to improve its corrosion and wear resistance [158, 159]. The bilayered nanoceramic coating presented significantly higher corrosion resistance in Hank's solution and wear resistance in SBF solution attributed to the presence of a large number of melted particles compared to other ceramics where they presented unmelted and melted particles, lower porosity and higher hardness for bilayered nanoceramic coating compared to other samples.

Titanium nitride (TiN) coatings by PVD, plasma nitriding, sputtering, gas nitriding, plasma immersion ion implantation, and ion implantation treatments have been widely used to improve the corrosion and wear behaviour along with the bioactivity of metallic materials. TiN has attracted attention due to its excellent properties such as high hardness, chemical stability, biocompatibility, haemocompatibility, high wear, and abrasion resistance. Because of these unique properties, TiN has been used on various applications such as dental prostheses, orthopaedic implants (hip, knee, ankle joint), heart valve prostheses, and dental surgery tools. The structure and biological properties of nitrogen treatment on different β-Ti alloys have been investigated [160–174]. Mohan et al. [174] performed a plasma nitriding treatment on Ti–15Mo–3Nb–3Al–0.2Si alloy using inductively coupled RF plasma and studied the corrosion behaviour by electrochemical impedance spectroscopy (EIS), potentiodynamic polarization, and immersion studies in Hank's solution. It was found that the surface hardness of the nitrided samples increased with increasing annealing temperature and hydrogen dilution. Although nitrided surfaces presented lower corrosion resistance, nitrided samples with hydrogen dilution displayed higher potential for apatite growth compared to that of the sample nitrided with 100% nitrogen and the uncoated one. Gordin et al. [173] implanted nitrogen into Ti–25Ta–25Nb β-type alloy using an original ion implantation technique based on the use of an electron cyclotron resonance ion source to produce a multi-energetic ion beam from multi-charged ions. The corrosion resistance of the nitrogen implanted Ti alloy was evaluated in SBF complemented by in vitro cytocompatibility tests on human foetal osteoblasts. It was found lower corrosion and ion release rate for the nitrogen implanted surface than for the non-implanted one whereas in vitro tests revealed a good level of cytocompatibility for both non-treated and nitrogen implanted Ti–25Ta–25Nb alloy. A high temperature gas nitrided Ti–27Nb alloy also presented significantly better corrosion resistance than the cp-Ti and untreated Ti–27Nb alloy in artificial saliva for different pH values, together with a good level of bioactivity [160, 167]. In wear point of view, the ion implantations, plasma nitrided and gas nitrided methods are more beneficial than the PVD techniques and sputtering mainly due to the formation of a gradient hardened layer and the good bonding strength of the nitrided layer resulted from the diffusion of nitrogen ions. For instance, the dense TiN coating deposited by sputtering presented lower wear resistance as compared to a compact plasma nitrided layer associated with the hard compound layer maintaining its integrity with the hardened nitrogen diffusion zone during the wear test [164]. While nitriding improves the corrosion and wear resistance, gas nitriding in high temperature is reported to cause low fatigue strength due to severe grain coarsening [161]. A possible approach to improve the tribological behaviour of the protective coatings can be achieved by increasing fracture toughness and hardness with the replacement of monolayered coatings by multilayers. The multi-layered TiAlN/CrN coatings on Ti–45Nb alloy presented better wear resistance than the monolayered CrN and TiAlN coatings in dry sliding condition attributed to their small grain size, high surface hardness and adhesion resistance [165].

Another approach studied in the literature to improve the corrosion and wear behaviour of β-Ti surface is oxygen treatment using plasma immersion ion implantation. Mohan and Anandan [175] implanted oxygen ions into Ti–13Nb–13Zr β-type alloy by plasma immersion ion implantation and investigated the influence of oxygen ion implantation on the apatite growth and corrosion behaviour in Hanks' solution. Results showed that the implanted samples had a higher potential for inducing apatite growth as compared to the untreated samples. Furthermore, the authors stated based on potentiodynamic polarization and EIS studies that the implanted layer behaved like a near-ideal capacitor with better passivation behaviour which can help in preventing the release of metallic ions from the implant material. Furthermore, the implanted surfaces displayed a lower coefficient

of friction during dry sliding wear tests, as compared to the untreated samples.

2.3 Chemical Surface Treatments

Chemical methods are attracting more attention owing to their lower cost, easier control and stronger adhesion between bones and implant surfaces compared to the samples treated by mechanical and physical methods. Through chemical surface modification, it is possible to provide direct bonding between bone and the implant. Chemical surface treatments can be used to generate a nanopatterned surface topography which is expected to be promising for the stimulation of bone tissue growth (osteointegration of bone tissue) [176]. Acid treatment (HCl, H_2SO_4, HNO_3, and HF, or a combination of them) is often used to remove the undesired material, to create a rough surface, and to obtain clean and uniform surface finishes. The schematic representation of chemical treatments and representative treated surfaces is given in Fig. 6, and the overview of chemical methods of β-Ti alloys are given in Table 3.

Acid treatments commonly performed to clean metallic surfaces or surface roughening to improve bonding quality of next coating layer or improve bioactivity of surfaces. The Ti–45Nb alloy surface modified by sandblasting, followed by acid etching in different solutions, chemical treated in H_2SO_4:H_2O_2 (volume ratio of 1:1; piranha solution) with ice cooling resulted with a nanopatterned surface that stated by the authors to be expected to stimulate bone cell interactions [92]. It has been reported significantly prolonged etching duration for Ti–Nb alloy compared to cp-Ti and Ti–6Al–4 V attributed to the excellent chemical stability of Nb. Chemically treated Ti–40Nb alloy by piranha solution enhanced the adhesion and spreading of human mesenchymal stromal cells, together with better metabolic and enzyme activity [177]. However, chemically treated Ti–45Nb alloy presented lower corrosion resistance than untreated alloy due to the alterations on the surface chemistry and increase on the exposure area resulted from nanopatterning. Müller et al. [178] investigated the influence of different acid–alkali treatments on Ti–13Nb–13Zr alloy produced by powder metallurgy (P/M). The authors evaluated the rate of hydroxy carbonated apatite (HCA) formation during in vitro bioactivity tests in SBF. After etching the samples by HCl, HF/HNO_3/H_2O (1:6:18), H_3PO_4, and then soaked in 10 M NaOH

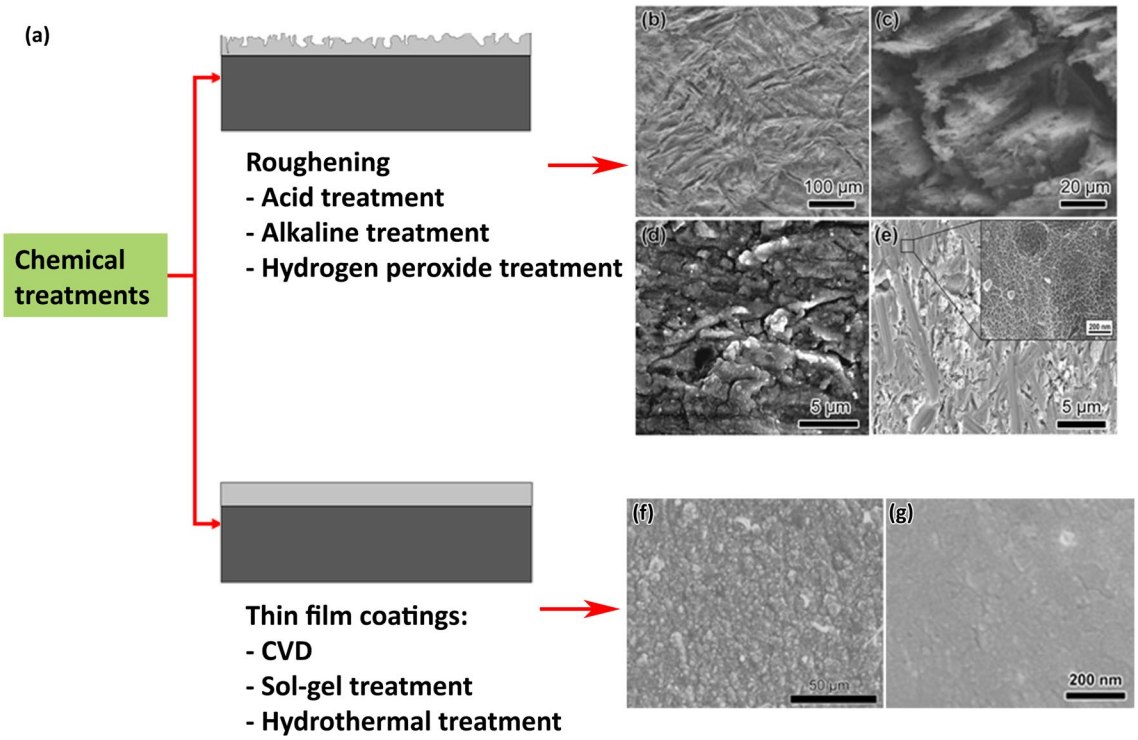

Fig. 6 **a** Schematic representation of chemical treatment process and representative treated surface SEM images of **b** HCl etched and **c** subsequently immersed in NaOH surfaces of Ti–13Nb–13Zr alloy (adapted from [178] with permission from Elsevier); SEM images of **d** NaOH treated and **e** piranha etched surfaces of Ti–40Nb alloy (adapted from [180] with permission from Elsevier); **f** representative SEM image of HA-coated surface on Ti–29Nb–13Ta–4.6Zr by MOCVD (adapted from [192] with permission from Elsevier); **g** SEM image of a treated Ti–24Nb–4Zr–8Sn alloy surface in saturated $Ca(OH)_2$ solution boiled for 30 min (adapted from [195] with permission from Elsevier)

Table 3 Overview of chemical surface modification methods applied for β-Ti alloys

Methods	Objectives	Alloys
Acid treatment Alkaline treatment Hydrogen peroxide treatment	Removing oxide scales and contamination Improving biocompatibility, bioactivity or bone conductivity	Ti–40Nb [177, 180, 305] Ti–45Nb [92, 306] Ti–13Nb–13Zr [178, 187] Ti–15Mo–5Zr–3Al [179] Ti–15Zr–4Nb–4Ta [179] Ti–35Nb–10Ta–1.5Fe [307] Ti–27Nb–13Zr [308] Ti–29Nb–13Ta–4.6Zr [183, 184, 190, 191, 309] Ti–24Nb–4Zr–8Sn [189, 252] Ti–5Mo–3Fe [186] Ti–20Nb–13Zr [310] Ti–15Mo [185] Ti–16In–3Nb–4Ta [181]
Sol–gel treatment		Ti–29Nb–13Ta–4.6Zr [311–314] Ti–15Mo [315]
CVD	Improving wear resistance, corrosion resistance and blood compatibility	Ti–29Nb–13Ta–4.6Zr [192] Ti–13Nb–13Zr [316, 317] Ti–12Mo–6Zr–2Fe [318]
Hydrothermal treatment	Improving hard tissue compatibility	Ti–30Nb–1Fe–1Hf [210, 215] Ti–29Nb–13Ta–4.6Zr [193] Ti–13Cr–1Fe–3Al [193] Ti24Nb–4Zr–7.9Sn [194, 195] Ti–25Nb–3Mo–3Zr–2Sn [196, 319]

aqueous solution, the authors reported that the rate of HCA formation was the highest for the samples etched in HCl.

As abovementioned, HA has excellent bioactivity, but its application has been limited in clinics due to its poor mechanical properties. Hence, the formation of a dense and uniform bone-like apatite layer grown on Ti alloys through alkaline treatment and soaking in SBF has been attractively studied as an alternative to HA coating techniques. A schematic illustration of apatite formation mechanisms in SBF is given in Fig. 7. It may be expected that the precipitated apatite coatings from soaking in SBF will be close to that of the biological apatite presents in human bone, where the SBF solution reproduces the human blood plasma. After alkaline treatment, a ~ 1 μm thick unstable sodium titanate layer is formed, and using heat treatment it is converted to a denser and mechanically stable layer. Acid and heat treatment was not effective for inducing apatite formation on Ti-based alloy attributed to enriched/remained alloying elements on their surfaces [179]. Also, while the chemical pre-treatments of alloy surfaces have a slight impact on apatite morphology, they do not affect the deposition process and its phase composition [180]. As can be seen from Fig. 7, during SBF soaking, the Ti–OH groups are formed resulted from the exchanged Na^+ and H_3O^+ ions. The negatively charged Ti–OH groups are combined with positively charged Ca^{2+} ions through electrical force and form calcium titanate. Similarly, the positively charged surface combines with negatively charged phosphate ions to form amorphous calcium phosphate, and apatite grows on the surface spontaneously by consuming the calcium and phosphate ions. It is reported that apatite was grown more quickly on the β-Ti alloy than Ti–6Al–4V alloy [181].

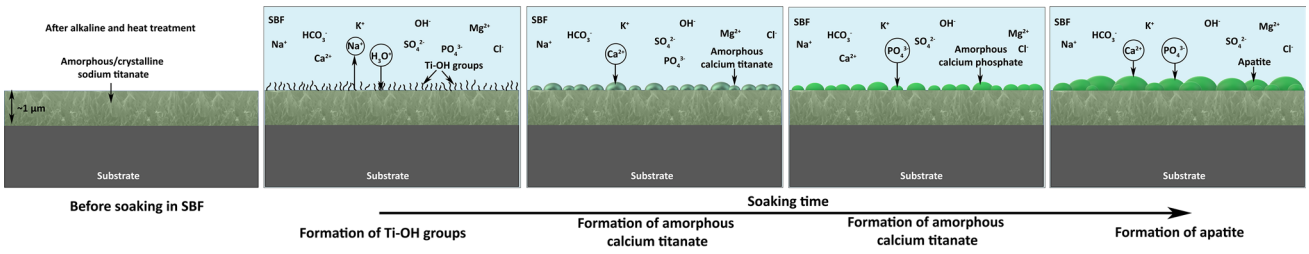

Fig. 7 Schematic illustration of the apatite formation mechanism on the surface of alkali and heat-treated Ti-based alloy soaked in SBF

The structure and bioactivity of alkali and heat treatment of β-Ti alloys have been investigated [180, 182–189]. Takematsu et al. [184, 190, 191] performed three different alkali solution treatments (electrochemical, hydrothermal, and hydrothermal-electrochemical) on Ti–29Nb–13Ta–4.6Zr alloy and compared the bioactivities and other characteristics of the modified surfaces. The authors showed the influence of the process to the surface morphology where electrochemical treatment resulted in a flat surface, hydrothermal treatment resulted in a smooth and fine mesh-like structure, and hydrothermal-electrochemical treatment led to a rough mesh-like structure. Moreover, apatite inductivity in SBF was reported to be influenced by surface roughness and chemical composition where increased roughness and decreased Nb content on the surface led to a higher apatite-induction ability. Also, the authors reported that a thicker oxide layer or presence of surface cracks decreased the adhesion strength, where cracks usually initiated as a result of thermal stress.

It has been reported that alkali [182] and alkali-hydrogen peroxide [185] treated Ti–15Mo alloy can induce bone-like apatite formation in vitro. The effect of alkali and hydrogen peroxide treatment on the electrochemical and biological performance of the Ti–5Mo–3Fe alloy surface was evaluated by Kumar et al. [186] and it was found that the alkali-treated alloy immersed in SBF solution exhibited notably higher corrosion resistance when compared with untreated and hydrogen peroxide treated samples. Furthermore, it was stated based on MG-63 in vitro cell culture studies that the alkali-treated samples showed better cell adhesion and spreading compared to the untreated and hydrogen peroxide treated samples. Zheng et al. [189] performed alkali treatment for calcium phosphate coatings on Ti–24Nb–4Zr–7.6Sn alloy and determined the adhesion and proliferation of rat osteoblast. The authors found that both the adhesion and proliferation of osteoblast cells on apatite formed Ti–24Nb–4Zr–7.6Sn were much better than on uncoated Ti–24Nb–4Zr–7.6Sn and cp-Ti.

Surface treatments with acid, alkali, hydrogen peroxide, and mechanical polishing, or a combination of these treatments are being applied to improve the adhesive strength of HA films [180]. Studies showed that the adhesive strength of such films can be improved by increasing the roughness of the underlying substrate. Hieda et al. [192] investigated the effect of acid treatment and mechanical polishing treatments on the adhesive strength of HA films deposited on Ti–29Nb–13Ta–4.6Zr alloy through metal–organic chemical vapor deposition (MOCVD) to increase the hard tissue compatibility. The authors reported that the adhesive strength of the HA layers formed on Ti–29Nb–13Ta–4.6Zr substrates treated with an HF solution significantly increased as compared to that of the HA film deposited on a polished Ti–29Nb–13Ta–4.6Zr surface. Also, the HA films on Ti–29Nb–13Ta–4.6Zr substrates treated with an H_2SO_4 solution exhibited lower adhesive strength than HA films on Ti–29Nb–13Ta–4.6Zr substrates treated with HF solution, regardless of the surface roughness of the substrates. Additionally, it was reported that the nanoscale surface asperities contributed to the adhesive strength, which was not observed for macroscale asperities.

The hydrothermal method is found to be very useful due to the formation of uniform coatings on complicated shapes, low processing temperature, low cost, and particularly because of strengthening the adhesion between the resultant coating and substrate. The surface wettability of implants is a crucial factor in their osteoconductivity because it influences the adsorption of cell-attached proteins onto the surface. In this respect, Zuldesmi et al. [193] compared the polished, hydrothermal treated, and anodic treated surfaces of Ti and four different Ti alloys (Ti–6Al–4V, Ti–6Al–7Nb, Ti–29Nb–13Ta–4.6Zr, and Ti–13Cr–1Fe–3Al). Hydrothermal treatment was performed in distilled water at 180 °C for 3 h whereas anodic treatment was performed in 0.1 M H_3PO_4 solution by applying potentials from 0 to 150 V with 0.1 V s^{-1} scanning rate. It was found that hydrothermal treatment increased the surface hydrophilicity of all types of Ti alloys and the osteoconductivity of Ti alloys after hydrothermal treatment and immersion in phosphate-buffered saline solution increased five times compared with that of the untreated samples.

Nanostructured TiO_2 coatings are found to be favourable for the early osteointegration and biocompatibility due to their bioactivity. Liu et al. [194] studied the biocompatibility and early osteointegration of nano-TiO_2 hydrothermally coated Ti–24Nb–4Zr–7.9Sn alloy compared with those of uncoated Ti-2448. The biocompatibility was evaluated using MTT assays, the histocompatibility was determined by observing the histological sections stained with HE (subcutaneous implantation, endosseous implantation), and the early osteointegration was tested using the alkaline phosphatase (ALP) activity and TGF-β1 expression. The authors reported an enhanced proliferation and cytocompatibility on the functionalized surfaces based on the MTT results, and better histocompatibility of the subcutaneous and endosseous implantation based on the in vivo studies. Zheng et al. [195] studied the functionalization of Ti–24Nb–4Zr–7.9Sn alloy by thermal treatment followed by hydrothermal treatments in supersaturated $Ca(OH)_2$ solution. The treatment resulted in a layer containing $CaTiO_3$, $CaCO_3$, $Ca(OH)_2$, and TiO_2, and the authors reported a formation of Ca–P layer after soaking in SBF for 3 days. Tao et al. [196] investigated the surface properties of the Ti–25Nb–3Zr–2Sn–3Mo alloy after functionalization by a hydrothermal treatment in urea solution at temperatures varying between 105 and 170 °C, followed by a heat treatment at 400 °C. The authors showed

that changes in temperature on hydrothermal treatment affected the surface structure where nanosheet films of ammonium titanate were observed after the treatment at 105 and 120 °C, whereas nanoparticle film of anatase TiO_2 containing Nb_2O_5 was formed at 150 °C. Moreover, the authors reported enhanced hydrophilicity on the functionalized surfaces after water contact angle measurements around 68° and 10° for untreated and treated alloys, respectively.

2.4 Electrochemical Surface Treatments

Electrochemical processes are performed by chemical action on the metal surface under an electric current passing through an electrolyte. The electrochemical setup and the examples of resultant porous with volcano-like structure, nanotubular, and HA-containing layers are presented in Fig. 8. These methods are simple and cost-effective, allowing the incorporation of bioactive elements, and can increase the corrosion resistance of the modified materials owing to a more stable and thicker oxide layer formed on the surface [197]. Oxide layers with different morphologies, thickness, roughness, wettability, chemical compositions, and crystalline structures are formed on the substrates depending on the applied voltage and electrolyte composition [198].

2.4.1 MAO

MAO treatment has been used by several authors to modify the surfaces of Ti and its alloys for several biomedical applications. Rafieerad et al. [199] reviewed the surface characteristics and corrosion behaviour of calcium phosphate-based composite layers on Ti and its alloys via MAO treatment. The authors concluded that the fabrication of bioactive surfaces to improve the osteointegration of Ti-based implants is strongly recommended via MAO treatment. It is possible to obtain different morphologies, microstructures, thickness, and crystalline structures of the anodic layers using different electrolytes, voltages, currents or treatment time. Furthermore, this type of treatment allows the incorporation of bioactive elements such as Ca and/or P using electrolytes such as $Ca(H_2PO_2)_2$ [197, 200–206], H_3PO_4 [200, 204, 206, 207] or a mixture of both [200, 208], calcium acetate (CA) [209–215], a mixture of CA and β-glycerophosphate (β-GP) [211, 212, 214–216], and NaH_2PO_4 [217]. Apart from bioactive elements, MAO also allows the incorporation of antimicrobial elements, such as Ag, Cu or Zn [218]. Some authors had reported the possibility of incorporation of bioactive additives into Ti-based alloys MAO layers such as tricalcium

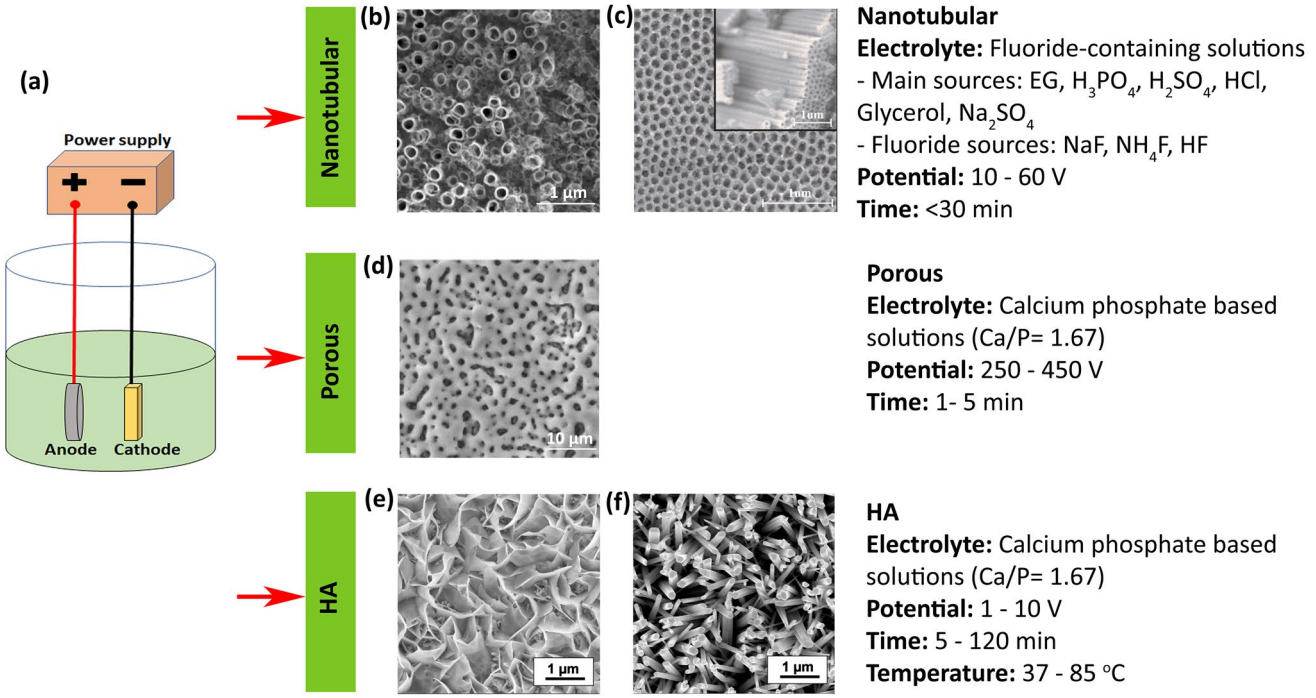

Fig. 8 **a** Schematic representation of the electrochemical surface modification set up, and the representative resultant surfaces with process parameters: **b** nanopores (adapted from [225] with permission from Elsevier, **c** nanotubes (adapted from [295] with permission from Elsevier), **d** porous oxide layer formed by MAO (adapted from [209] with permission from Elsevier), **e** plate-like HA, and **f** needle-like HA (adapted from [180] with permission from Elsevier)

phosphate (TCP, $Ca_3(PO_4)_2$), wollastonite ($CaSiO_3$) or SiO_2 particles which are known to enhance osteointegration [197, 201–205].

Simka et al. [200] and Kasek-Kesik et al. [201, 202] treated β-Ti alloy (Ti–15Mo) via MAO. The authors used H_3PO_4, $Ca(H_2PO_2)_2$ or $(HCOO)_2Ca$ as an electrolyte and observed that the morphology and chemical composition of the anodic layers were strongly dependent on the applied voltage and chemical composition of the electrolyte used during the treatment. Independently of the electrolyte, when the voltage increased, the pore size of the anodic layers increased, however, more cracks were observed. The incorporation of Ca and/or P was, as well, dependent on the applied voltage. Moreover, the thickness of the anodic layers was dependent on both applied voltage and electrolyte concentration. For example, thicker anodic layers were observed for the highest concentration of $(HCOO)_2Ca$. MAO parameters or electrolyte concentrations also influence the crystalline structure of the anodic layers. Simka et al. [200] found only a single crystalline phase TiO_2 after treatment in a mixture of $Ca(H_2PO_2)_2$ and H_3PO_4 electrolytes, indicating that TiO_2 layers were amorphous. However, after decreasing the concentration of $Ca(H_2PO_2)_2$, the authors reported the existence of the anatase phase.

Kazek-Kesik et al. [201, 205] used $Ca(H_2PO_2)_2$ as electrolyte together with TCP, wollastonite or silica particles. The authors stated that the particles from the electrolyte suspension were successfully incorporated into the porous anodic layers for voltages higher than 150 V. However, while increased concentrations of TCP and wollastonite led to an increase in Ca and P incorporation the opposite was observed on the increased silica particle addition. Regarding the surface roughness, no significant influence was found when wollastonite or silica particles were used. However, the highest roughness value was found for the highest concentration of TCP particles. Kazek-Kesik et al. [202] also compared the influence of the substrate (Ti–6Al–7Nb, Ti–13Nb–13Zr and Ti–15Mo) on their anodic layer characteristics after MAO treatment. The authors added TCP particles into $Ca(H_2PO_2)_2$ electrolyte for MAO treatment and observed that TCP particles were mainly deposited on the top of the anodic layers and filled the pores of the outer porous layer. Moreover, the formed oxide layers were different in terms of thickness, roughness, chemical composition, and crystalline structures, depending on the substrate. As well, their total thickness increased significantly with the incorporation of TCP particles. Oppositely, the roughness of the anodic layer with TCP particles decreased when compared with only anodized titanium alloys leading to an influence on the wettability. Bio-functionalization of Ti–13Nb–13Zr surface via MAO was studied by Kazek-Kesik et al. [197, 219] using a $Ca(H_2PO_2)_2$ electrolyte with the addition of TCP, wollastonite or silica particles where the microstructures and chemical composition of the anodic layers were strongly dependent on the applied voltage. Moreover, the final surface roughness reported to be increased after the treatment.

Another β-Ti alloy that had been treated by the MAO process is Ti–30Nb–1Fe–1Hf [210, 214, 215]. Ou et al. [210, 215] used a calcium acetate (CA) and β-GP mixture as an MAO electrolyte and reported a three-layer structure, namely, an amorphous and crystalline outmost porous layer followed by an inner layer with several pores, and finally a thin and compact layer. Moreover, the presence of Nb promoted the formation of the amorphous phase of the anodic layer. Oppositely to cp-Ti, when the voltages on MAO treatment increased, the crystallinity of the anodic layers decreased on Ti–Nb alloys. The incorporation of Ca and P was also succeeded with a Ca/P ratio maximum of 1.91 depending on MAO parameters. On the other hand, Pan et al. [214] used similar electrolyte to modify the surface of the same alloy and reported that the presence of Nb in Ti alloy can promote both layer rupture voltage and dielectric breakdown voltage due to the mixture of oxides (Ti and Nb oxides) that are known to stabilize the amorphous structure and delay oxygen generation.

Gebert et al. [220] used a NaOH alkaline solution as electrolyte during the MAO process and reported surfaces having a compact and thin inner layer followed by a much thicker outer layer with micro-pores and micro-channels. Moreover, the presence of Nb enhanced the thickness growth of the outer layer. On the other hand, Sharkeev et al. [207] performed MAO treatment on Ti–40Nb using a mixture of H_3PO_4, biological HA, and calcium carbonate. The authors pointed the need for performing crystallization annealing treatment after the MAO process to obtain a crystalline structure on the anodic layer. The anodic layer was formed by a thin compact oxide layer, intermediate sublayer, and the typical porous CaP layer. As the voltage of MAO treatment increased, the thickness of the anodic layer also increased linearly from 35 to 90 µm. Moreover, when the voltage ranged between 200 and 300 V, the CaP layer presented spheres and pores. However, when the voltage increased up to 400 V, the transformation of micro-arc discharges into arcs caused the destruction and fragmentation of the spheres leading to a decrease of the anodic layer porosity. By using voltages under 200 V, XRD analysis just showed intense peaks of Ti and Nb and poor reflexes of NbO_2 phases, mainly due to the small thickness of the anodic layer. The absence of TiO_2 phases into the anodic layers was explained by higher thermal conductivity and lower electrical resistivity as compared to Ti. When the process voltage increased up to 300 V, the anodic layer was formed by an amorphous phase and crystalline phases such as $CaHPO_4$ and β-$Ca_2P_2O_7$. Further increase on the process voltage up to 400 V led to a decrease

on the peak intensity of the characteristically crystalline phases of the anodic layers.

Tao et al. [209] studied the effect of Nb, Zr, and Sn on the characteristics of the anodic layers formed by MAO. The authors used a CA electrolyte with an applied voltage of 250 V and after the samples were heat-treated at 600 °C for 1 h in air. The anodic layer porosity increased with increasing voltage, and at 250 V, the porous structure covered uniformly all the surfaces. Although the surface roughness increased with the working voltage, it was not affected by the heat treatment. After heat treatment, the anodic layers were mainly composed of TiO_2 (anatase and rutile), Nb_2O_5, CaO, and SnO_2. However, the diffraction intensity of Nb_2O_5, CaO, and rutile increased after heat treatment. A study using the same alloy was reported by Gao et al. [213] where the authors also used the similar MAO treatment parameters. However, XRD analysis only detected Ti, anatase and rutile peaks while elements such as Ca, Nb, Zr, and Sn were only detected by EDS analysis. These results showed the importance of the post-heat treatment on the crystallinity of the anodic layers as reported by Tao et al. [209].

Other alloys as TiZrSnMoNb [211, 212], TiAlNb [202], TiCrAlFe [217] have also been modified by MAO. However, the effect of the alloying elements on the MAO treatment of the new alloys is yet to be fully understood. Besides, although the MAO process has been successfully used to modify β-Ti alloy surfaces mainly to increase the bioactivity, very little is known on the growth mechanisms of MAO layers including the incorporation process of the bioactive elements.

Apatite forming ability has been used to access the bioactivity, however, apatite forming ability depends not only on the chemical composition of the anodic layers but also on the volume of SBF solution used during the soaking process. Thus, due to these factors, different results are reported in the literature. Kasek-Kesik et al. [204] reported that according to the mechanism of apatite crystallization, the presence of anatase and rutile may be negatively charged in SBF and adsorbs Ca^{2+} ions. Ca^{2+} ions also attract OH^- and HPO_4^{2-} groups. If an anodic layer does not have phosphorous compounds, the formation of apatite may be delayed or not exist, however, it is still possible by the formation of calcium titanate ($CaTiO_3$) on the anodic layer since the presence of $CaTiO_3$ facilitates the adsorption of hydroxyl radicals and phosphate leading to the formation of apatite.

Several authors reported that apatite forming ability is induced on MAO-treated surfaces of β-Ti alloys, independently of the chemical composition of the substrate [204, 206, 209, 212]. Tao et al. [209] concluded that a heat treatment after MAO on Ti–24Nb–7Zr–7.9Sn alloy improved the apatite forming ability. The same behaviour was described by Kazek-Kesik et al. [204] for Ti–15Mo alloy treated by MAO and post-treated by heat treatment. On the other hand, Yu et al. [212] reported that in situ formation of apatite on the MAO-treated surfaces of Ti–3Zr–2Sn–3Mo–25Nb in SBF was related to Ca- and P-containing compounds. Moreover, apatite nuclei were formed after approximately 14 days of immersion and it continued to grow, firstly filling the pores and after spreading over the entire surface. Sowa et al. [206] modified surfaces of Ti–13Nb–13Zr alloy by MAO and the authors were able to detect small amounts of apatite precipitates formed on the modified Ti alloy surface after immersion in SBF, although the treated surfaces presented Ca/P ratios bellow 1.67 (Ca/P atomic ratio of stoichiometric HA).

Immersion of MAO-treated surfaces in SBF to promote apatite forming ability and thus bioactivity has been widely studied. However, the reliability of evaluation of bioactivity of those surfaces by simply immersing in SBF has been criticized due to the lack of proteins presence or bacterial activity. Thus, in vitro and/or in vivo studies have been reported to access the biological response of the modified surfaces. Kazek-Kesik et al. [202] developed multi-layered surfaces by electrophoretic deposition of TCP particles on MAO-treated surfaces of V-free alloy (Ti–6Al–7Nb, Ti–13Nb–13Zr, and Ti–15Mo). The number of incorporated TCP particles was higher for Ti–13Nb–13Zr and Ti–15Mo alloys than for Ti–6Al–7Nb. The adhesion and number of MG-63 osteoblast-like cells were investigated by Kazek-Kesik et al. [202] and it was observed that independently of the base alloy, none of the modified surfaces were cytotoxic. The highest biological activity was found for MAO + TCP treated Ti–15Mo alloy, while the surface modification did not significantly influence the cell proliferation on Ti–6Al–7Nb and Ti–13Nb–13Zr alloys. On the other hand, another study from the Kazek-Kesik et al. [204] modified Ti–15Mo alloy by MAO and showed that after 5 days of culture, hBMSC cells have well adhered to all modified surfaces. However, the anodic layers with the highest atomic ratio of Ti/Ca presented higher ALP activity, collagen production, and mineralization when compared with the untreated alloy. Moreover, these surfaces showed only a single strain of attached *D. desulfuricans* bacteria and it was not observed the formation of bacteria biofilm. Furthermore, the Zn, Cu, and Ag-doped CaP MAO composite was formed on Ti–40Nb alloy, presented an improvement on the antibacterial activity [221].

The biological performance of low Young's modulus Ti–24Nb–4Zr–7.9Sn alloy bio-functionalized by MAO has been reported [209, 213]. After heat treatment, the anodic layers consisted of TiO_2, CaO, Nb_2O_5, and SnO_2. In vitro studies on rabbit's osteoblast showed a considerable improvement in cell proliferation due to the increased roughness of the surfaces but as well due to the incorporation of Ca into the anodic layers [209]. Although no heat treatment was performed after MAO, Gao et al. [213] showed that MAO-treated surfaces presented significantly higher

absorbance of cells when compared to the untreated alloy. Moreover, the porous structure and chemistry of the anodic layers led to a stronger and faster bone response of the modified surfaces.

Ou et al. [215] functionalized Ti–30Nb–1Fe–1Hf alloy by MAO using a Ca- and P-rich electrolyte followed by a post hydrothermal treatment. In vitro studies with MG-63 cells indicated no significant differences between the untreated and treated alloy on optical cell density and ALP activity. However, cell adhesion and cell spreading were reported to be improved by hydrothermal treatment. Sowa et al. [206, 222] modified Ti–13Nb–13Zr alloy by MAO in an electrolyte containing Ca and P elements. The authors observed that the incorporation of Ca and P into the anodic layer enhanced the differentiation of hBMCs into osteoblasts. Moreover, the increased roughness after MAO promoted cell spreading. A similar improvement was achieved for Ti–45Nb alloy through 26 days of cell culture [223].

Bioactive surfaces were produced by Zhao et al. [211] on Ti–5Zr–3Sn–5Mo–15Nb alloy using MAO where better osteoblasts adhesion, spread, viability, and differentiation were observed. However, by increasing the applied voltage of MAO treatment, better cell spread and viability was observed. The authors stated that this behaviour might be explained by the increased roughness together with an increased Ca/P ratio obtained at the highest voltage. On the other hand, Yu et al. [212] used similar alloy and MAO treatment conditions but performed further activation in an aminated solution. Results showed that MC3T3-E1 cell proliferation was favoured and hard tissue implantation indicated that the activated surfaces exhibited good biocompatibility and better osteointegration than the untreated alloy. Chen et al. [217] bio-functionalized Ti–13Cr–3Al–1Fe alloy using MAO in NaH_2PO_4 electrolyte. In vitro tests using MC3T3-E1 cell line and in vivo tests in distal femora of Japanese white rabbits showed that the rutile-rich TiO_2 layer gave better biocompatibility and osteointegration performance than anatase rich phase, suggesting that MAO-treated implant may achieve better bone formation and on growth.

In addition to their increased bioactivity, anodic layers on Ti-based alloy created by MAO can also increase the corrosion resistance of the base alloys. Kazek-Kesik et al. [197, 201, 202, 219] reported the corrosion behaviour of different low Young's modulus alloys modified by MAO. The corrosion behaviour of Ti–6Al–7Nb, Ti–13Nb–13Zr, and Ti15Mo MAO-treated alloys was studied in Ringer's solution [202]. Surface modification caused an increase in the corrosion resistance for all substrates. However, the highest differences in the electrochemical parameters were found between treated and untreated Ti–15Mo alloy.

It has been reported [201] that MAO treatment in TCP, wollastonite or silica particle-containing electrolytes improved the corrosion resistance of Ti–15Mo alloy due to the barrier-type oxide layer formed on the alloy surface. The highest corrosion resistance was recorded for the electrolyte containing TCP particles owing to the thicker and more compact oxide layer. Similar MAO treatment was performed on Ti–13Nb–13Zr by Kazek-Kesik et al. [197, 219]. Results showed that the OCP values in Ringer's solution were much nobler on the treated samples, showing a lower tendency to corrosion when compared with the untreated alloy. Furthermore, the polarization resistance increased and current density decreased, independently of the incorporated particles, as compared to the untreated alloy [197]. By immersing the treated alloy in Ringer's solution for 5 months, the authors could observe the degradation of the anodic layers due to the dissolution of Ti, Nb, and Zr phases [219]. The concentration of dissolved Ti ions in electrolyte was found to be influenced by the applied voltage during MAO treatment as a consequence of increased surface roughness with increasing applied potential. Apart from Ti ions, Nb and Zr ions were also detected but their amounts were very small.

2.4.2 Nanotubular Structures

TiO_2 nanotubular surface structures have been widely reported for biomedical applications since protective stable oxides on Ti-base surfaces lead to a favourable osteointegration [201, 224]. TiO_2 nanotube growth is obtained by anodic treatment using F^- containing electrolytes. The nanotube growth has been reported on binary, ternary and quaternary β-Ti alloys such as Ti–Nb [220, 224], Ti–13Zr–13Nb [225, 226], Ti–25Ta–*x*Zr [227], Ti–35Nb–*x*Zr [228, 229], Ti–29Nb–13Ta–4.6Zr [230], and Ti–24Nb–4Zr–7.9Sn [231, 232].

Gebert et al. [220] compared the growth of the nanotubes on Ti–40Nb and cp-Ti (grade 2) in fluoride-containing solutions and observed a similar growth. Moreover, the oxide nanotubes presented amorphous structures and mixed compositions as $(Ti_xNb_{1-x})O_2$. On the other hand, Jang et al. [224] produced nanotubular surfaces on Ti–*x*Nb ($x = 10$, 20, 30 and 40 wt%) alloys using 1.0 M H_3PO_4 electrolyte containing 0.8 wt% NaF. The nanotubes formed on the Ti–*x*Nb alloy surface presented a wide range of diameters (55–220 nm). More specifically, as Nb content increased, the length of the nanotubes increased from 730 nm to 2 µm. The authors also reported that the initial structure of the nanotubes was an amorphous TiO_2–Nb_2O_5 layer. After annealing at 300 and 450 °C, the formation of crystalline anatase, and after annealing at 600 °C, in addition to anatase, the formation of rutile was detected.

Ossowska et al. [225] and Hernández-López et al. [226] performed anodic treatment to obtain nanotubes on Ti–13Zr–13Nb alloy using a mixture of 1 M H_2SO_4 and 0.035 M HF. Hernández-López et al. [226] stated that shorter anodizing times resulted in nanostructured layers

with a porous morphology, whereas after longer anodizing times, the anodic film showed a nanotubular structure. Moreover, the average molecular composition given by Rutherford backscattering spectroscopy (RBS) analysis was $(TiNbZrO)_{0.45}0.081TiF_4 0.102NbF_5 0.081ZrF_4$ for the nanoporous layers while the nanotubular layers presented a molecular composition as $(TiNbZrO)_{0.61}0.078TiF_4 0.098NbF_5 0.078ZrF_4$. On the other hand, Ossowska et al. [225] compared the nanotube growth on dense and porous Ti–13Zr–13Nb alloy. Results showed a fine nanotubular structure with long nanotubes, moreover, the nanotubular structure is formed also inside the pores in the case of the porous alloy. However, the nanotube dimension was smaller on the porous alloy when compared to the dense alloy.

Li et al. [231] and Hao et al. [232] modified the surface of Ti–24Nb–4Zr–8Sn by anodic treatment. Both authors performed the anodic treatment in a neutral electrolyte with 1 M $(NH_4)_2SO_4$ and 0.15 M NH_4F. Hao et al. [232] stated that the outer diameter of the nanotubes increased from 30 to 90 nm as the treatment voltage increased from 10 to 25 V. Results showed that the contact angle decreased sharply with increased nanotube diameters from 30 to 70 nm and then was constant with the further increase of diameter to 90 nm. The authors suggested that the surface energy increases with an increase of nanotube diameter up to 70 nm, which was explained by the formation of surface oxides and their contribution to surface roughness. XPS analysis showed that the outmost nanotubular layer consisted of amorphous mixed oxides of TiO_2, Nb_2O_5, SnO_2, and ZrO_2. Similar results regarding the chemical composition of the oxides were also reported by Li et al. [231].

Similar to MAO-treated β-Ti alloys, studies investigating the corrosion behaviour of nanostructured surfaces on β-Ti alloys are scarce. Jang et al. [224] performed potentiodynamic polarization tests in 9 g/L NaCl at 36.5 ± 1 °C for nanotubes formed on Ti–*x*Nb alloys and found that the corrosion resistance of nanotubular structured alloys was lower as compared to the untreated alloys. The authors explained this behaviour by the defected structure of the nanotubular surfaces that may promote the current transport. However, the anodic treated samples presented a wider range of a passive region when compared with the untreated alloys, suggesting that the mixture of TiO_2 and Nb_2O_5 film was more stable. On the other hand, Ossowska et al. [225] and Hernández-López et al. [226] reported that the proper formation of nanotubular structures by anodic treatment resulted with a better corrosion behaviour as compared to the bare alloy.

Nanotubular structures on ternary and quaternary β-Ti alloys have been reported to stimulate rapid cell proliferation and osteoblast differentiation as well as to accelerate osteointegration and facilitate the transport of nutrients and bone ingrowth [231, 232]. It has been shown that the formation of ordered nanotubes on Ti–24Nb–4Zr–7.9Sn alloy via anodic treatment improved cytocompatibility, as well, enhanced bone implant integration in vitro and in vivo [231]. Hao et al. [232] obtained nanotubular surfaces with mixed oxides (TiO_2, Nb_2O_5, SnO_2, and ZrO_2) and reported after biological studies with osteoblast-like MG-63 cells that smaller nanotube diameter was beneficial for the cell adhesion, proliferation, and differentiation. Also, the antibacterial behaviour of Ti–35Nb alloy was improved with the corporation of Sn as an alloying element [233].

2.4.3 HA Electrochemical Deposition

HA and calcium phosphate ceramic coatings are widely used in the biomedical field due to their excellent response to cell adhesion and proliferation, as well as their ability to enhance bone ingrowth and osteointegration processes. The deposition conditions have a great effect on the structure and biofunctionality of HA coatings. The electrochemical deposition of HA coatings on metallic biomaterials has unique advantages and it is an attractive technique because highly complex structures can be coated quickly at low temperatures. Moreover, the coating morphology and chemical composition of HA can be well controlled by varying the electrochemical potential, current, electrolyte concentration, and temperature.

Several studies reported the electrochemical deposition of HA [180, 210, 234–237]. Schmidt et al. [180] studied the influence of electrolyte temperature and different chemical pre-treatments on Ti–40Nb alloy for the deposition of the HA layer. The authors performed potentiostatic deposition of HA using a mixture of $Ca(NO_3)_2$ and $NH_4H_2PO_4$ on grounded surfaces, etched surfaces with piranha solution, and alkali-treated surfaces. The morphology of the HA deposit was dependent on the electrolyte temperature. When the electrolyte temperature increased from 60 to 80 °C, the morphology of HA passed from plate-like to needle-like shape. However, the use of different pre-treatments did not have a significant effect on HA layer morphology. On the other hand, Byeon et al. [237] performed HA deposition on Ti–*x*Nb alloy by cyclic voltammetry in two different electrolytes (CaP—a mixture of $Ca(NO_3)_2 4H_2O$ and NH_4PO_4; and Zn–CaP—a mixture of $Ca(NO_3)_2 4H_2O$, NH_4PO_4 and $Zn(NO_3)_2 4H_2O$). Although different Ca- and P- rich electrolytes were used, the Ca/P ratio kept constant, and the HA layer presented a nanoscale rod-like HA for CaP electrolyte, while the Zn–CaP electrolyte led to a nanoscale network-like Zn–HA layer. Although the authors reported successful Zn–HA layer deposition, further studies are needed to get a better understanding of the formation and properties of these layers on Ti–Nb alloys.

Kim et al. [234] used a mixture of $Ca(NO_3)_2$ and NH_4PO_4 as an electrolyte to deposit HA by cyclic voltammetry over nanotubular structured anodic layer on Ti–25Ta–*x*Zr alloy.

Although all the deposited surfaces showed a Ca/P ratio lower than 1.68, a successful HA layer was deposited on its surfaces. The HA precipitate morphology was influenced by the Zr content of the alloy; as the Zr content increased, HA precipitates morphology changed from plate-like or leaf-like shape to needle-like or flower-like shape. A similar electrolyte was used by Kim et al. [235] to deposit HA layers on highly ordered nanotubular surfaces of Ti–25Nb–*x*Hf alloys. The authors observed that the needle-like nucleation and growth of the HA particles were promoted on the increased number of cyclic voltammetry cycles. However, the morphology of HA precipitates was influenced by Nb and Hf contents.

A study on the electrochemical deposition of HA on nanotube-formed Ti–Nb–Zr alloys was reported by Jeong et al. [236]. The authors studied deposition protocols using 5, 10, and 30 cycles of the pulsed current method and two electrolytes based on a mixture of $Ca(NO_3)4H_2O$ and NH_4PO_4. The HA layer morphologies changed from a mixture of rough particles and plate-like shape particles to entirely plate-like shapes depending on the number of deposition cycles and the Ca and P concentrations in the electrolyte.

2.5 Laser Surface Treatments

Most of the laser surface treatments for β-Ti alloys were performed in a nitrogen-rich environment resulted in the nitrided surface. Laser nitrided Ti–20Nb–13Zr alloy presented significantly higher hardness, hydrophilicity, coefficient of friction, and corrosion resistance in artificial saliva and SBF compared to the untreated alloy, cp-Ti, and Ti–6Al–4V alloy due to formation of a uniform 9 µm thick nitrided layer [238, 239]. Similar behaviour was reported for different β-Ti alloys namely Ti–35Nb–7Zr–5Ta [240], Ti–45Nb [241], Ti–13Nb–13Zr [242], Ti–35Nb–2Ta–3Zr [243], Ti–35Nb–7Zr–5Ta [244], and Ti–35.3Nb–7.3Zr–5.7Ta [245]. Femtosecond lasers are being used to increase the surface roughness and reported to provide significant advantages for hole formation compared to nanosecond lasers. Its advantages are negligible heat transfer and the absence of a liquid phase since the vapor and plasma phase are formed very quickly. In addition to these advantages, the periodic nanostructures are self-organized in the laser-irradiated field. Jeong et al. [229] evaluated the nanotubular surfaces formed on the femtosecond laser-treated Ti–35Nb–*x*Zr ($x = 3$ and 15 wt%) and reported an extensive proliferation and spreading of the MG 63 cells. Similarly, laser treatment was reported as a sufficient pre-treatment for HA and β-TCP bio-ceramic coatings associated with the formation of oxides diversity and irregular morphology on Ti–15Nb alloy.

Saud et al. [246] investigated the microstructure, corrosion behaviour, bioactivity, and antibacterial activity of graphene oxide (GO) coated by dip coating on femtosecond laser surface modified Ti–30Nb alloy. The authors reported that laser-treated and GO-coated samples displayed higher corrosion resistance than the GO-coated and uncoated samples in SBF at 37 °C. Moreover, the GO coating on Ti–30Nb alloy led to a superior antibacterial activity against Gram-negative bacteria as compared with the uncoated samples. Similarly, fibre laser nitrided Ti–35Nb–7Zr–6Ta alloy drastically improved the mesenchymal stem cell attachment, proliferation and differentiation, and also led to a reduction on staphylococcus aureus bacterial attachment due to formation of a hard rough surface with low hydrophobicity [247, 248].

2.6 Immobilization of Biomolecules

Bioactive molecules are also used to enhance the soft tissue compatibility on metallic biomaterials. Many studies investigated the biopolymer coated cp-Ti and Ti–6Al–4V alloy, however, a very limited number of studies are available on biopolymer coated β-Ti alloys [188, 249–253]. The schematic diagram for the immobilization process is presented in Fig. 9. Biochemical modification of the Ti–25Nb–16Hf alloy with elastin-like polymers (ELPs) was performed, and their influence on the cell response was analyzed by González et al. [249]. ELPs presented remarkable biocompatibility and one of these polymers contains the well-known cell adhesion amino acid sequence, arginine-glycine-aspartic (RGD). It was found that the RGD interface presented enhanced results in terms of cell adhesion and spreading but no improvement was observed on the numbers and differentiation of the cultured cells. Hsu et al. [250] investigated the biocompatibility of NaOH treated Ti–25Nb–8Sn alloy surface and found that the RGD peptide grafted Ti–25Nb–8Sn alloy significantly enhanced the cell adhesion, proliferation, and differentiation.

Adhesiveness to metallic materials is an important issue for biomedical polymer coatings from the viewpoint of long-term durability. Silane-coupling treatment is a traditionally popular route for increasing the adhesive strength between metallic materials and polymers. Hieda et al. [251] investigated the effect of terminal functional groups and silane layer thickness on the adhesive strength of Ti–29Nb–13Ta–4.6Zr alloy to segment polyurethane (SPU) and reported that silane-coupling treatment led to a significant increase on the shear bond strength for all tested types of terminal functional groups and the silane layers thickness. Moreover, an immobilized 3-aminopropyltriethoxysilane-reduced graphene oxide (APTES-RGO) nano-layer coated on Ti–29Nb–13Ta–4.6Zr alloy presented better tribological behaviour as compared to the uncoated alloy [188].

2.7 Hybrid/Multi-layered Treatments

The hybrid treatments have been aimed to effectively enhance the mechanical and biological properties, and also

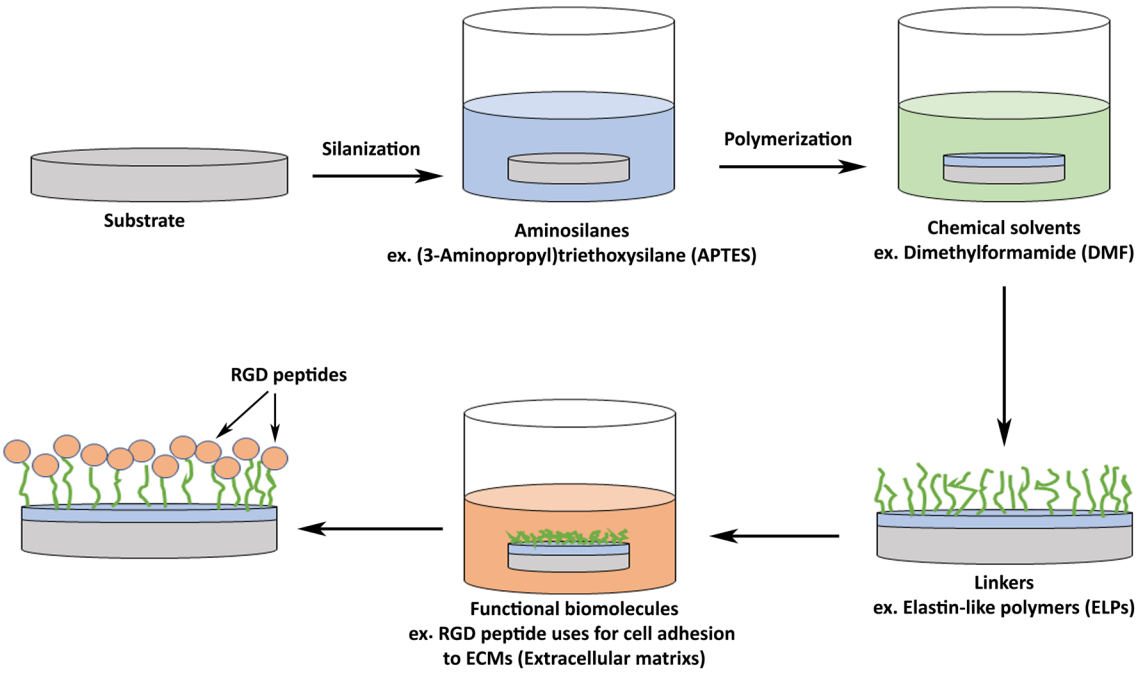

Fig. 9 Demonstration of the immobilization process of biomolecules on a bare surface

reduce the interfacial failure. Bio-functionalization of β-Ti alloys by combining different techniques are studied in the literature. Choe [254] developed a double-layered surface on Ti–30Nb–*x*Zr ($x=3$ and 15 wt%) having a nanotubular inner layer formed by anodic treatment and a HA outer layer formed by electron beam-physical vapor deposition (EB-PVD). The author investigated the corrosion behaviour of the functionalized surfaces in 9 g/L NaCl solution at body temperature and reported the spalling of the HA layer on the samples only coated with a single HA layer, and cracking of the HA layer on the double-layered surfaces due to the differences on the size of the nanotubes affected the corrosion behaviour mainly leading to the appearance of a breakdown potential on the passive region, which was not observed on the bare alloy. A similar double-layered structure was also developed by Jeong et al. [228] on Ti–35Nb–10Zr alloy having a femtosecond laser-treated surface to increase the roughness. The authors stated that the application of femtosecond laser-treated created microscale features can be beneficial for mechanical interlocking with bone. Moreover, based on the SEM observations, the authors reported a higher trend on the attachment and spreading of MG-63 cells on the double-layered surfaces developed on the femtosecond laser-treated alloy. Similar hybrid structure (NT + HA) was developed on Ti–25Nb–*x*Hf ($x=0$ and 7) [235], Ti–29Nb–*x*Zr ($x=3$ and 15) [236], Ti–25Ta–*x*Zr ($x=0$, 3, 7 and 15) [234], Ti–13Ta–2Mo–6Zr [255], and Ti–20Ta–1Mo–8Zr [255]. The authors reported that the HA structure was significantly influenced by morphology, diameter of tubes, and distribution of nanotubular layer, which were changing by microstructure and composition of the alloy. Apatite precipitation was also affected by nanotubes diameter, where the largest diameter presented better apatite formation for Ti–35Nb–2Zr–0.2O alloy [256]. In addition to biological improvement observed by in vitro studies, membranes treated by this hybrid structure on Ti–20Ta–1Mo–8Zr alloy were covered on rat calvarial defects, and tomography, histologic and fluorescent analysis indicated higher bone mineral density and a contact osseointegration, suggesting durable osteogenesis at the early stage of bone defect repair [255].

RF sputtered TiN coatings on nanotubular Ti–25Ta–*x*Zr alloys ($x=0$, 3, 7, and 15 wt%) were studied by Kim et al. [227]. The authors reported that as the Zr content in the alloys increased, the average thickness of the nanotubular layer increased. For the alloy with the highest Zr content, the nanotubular surfaces were covered entirely with the RF-sputtered TiN film. The authors concluded that the Zr content affected roughness and wettability, leading to highly hydrophilic properties on the nanotubular surfaces. As discussed in Sect. 2.6, the immobilization of bio-functional polymers is important for improving the tissue compatibility. A poly(sodium styrene sulfonate) (PNaSS) biopolymer grafted with nanotubular layer grown on Ti–15Mo and a significant improvement of bioactivity and decrease of bacterial adhesion was reported [257]. However, these polymers may not sufficiently adhere to metallic materials. Nanostructures (nanopores and nanotubes) were formed on

Ti–29Nb–13Ta–4.6Zr surfaces through anodic treatment to improve the adhesive strength of SPU [230]. It was found that the anchor effect given by the nanostructures increased the adhesive strength of SPU.

The MAO/HA structure is another commonly studied hybrid treatments for β-Ti alloys [210, 258–261]. Park et al. [258] electrochemically deposited HA on MAO layer grown on Ti–3Ta–xNb ($x = 0$ and 10), and it was found that the particle size and morphology of HA was affected by the composition of the alloy and alkaline treatment. Also, a biodegradable poly(lactide-co-glycolide) (PLGA) polymer was deposited on the MAO layer formed on the Ti–15Mo alloy [203]. Additionally, the PLGA loaded with the drug of amoxicillin layer was coated on MAO layer of Ti–15Mo using a dip coating technique, and it was reported an improvement on corrosion and bacterial resistance of substrate [261]. The main goal of the polymer-oxide layer was to explore the active substance to be released after implantation.

2.8 Other Methods

In the literature, other methods such as producing composite layers (metal matrix composite and HA biocomposite) or bioactive element addition were also studied. Xiaopeng et al. [262] produced Ti–35Nb–2.5Sn—15 wt% HA biocomposite with mechanical alloying followed by sintering under high vacuum at 1100 °C. The authors reported that the samples ball-milled during 4 h presented a relative density of 95.55% and Young's modulus of 20 GPa (defined by compressions tests). On the other hand, biological studies performed with MC-3T3 osteoblast-like cells revealed higher cell viability and proliferation. Majumdar et al. produced TiB in situ reinforced Ti–35Nb–5.7Ta–7.2Zr [263] and Ti–13Zr–13Nb [264] matrix composites with addition of 0.5 wt% B particle to improve the wear resistance, however, the biological studies performed with MG63 cells revealed a decreased cell proliferation on the in situ composites, which may be explained by cytotoxicity of B. For instance, Málek et al. [265] produced in situ TiB reinforced Ti–35Nb–6Ta matrix composites with 0.05, 0.1, 0.3 and 0.5 wt% B particle and claimed that 0.1% and higher B addition had a slightly adverse effect on cytotoxicity.

Ou et al. produced Ti–27.5Nb alloy with the addition of 0.2, 0.7 and 1.2 wt% Ag by arc melting to obtain antibacterial properties [266]. The authors did not observe any influence of Ag on the adhesion and proliferation of MG-63 and NIH-3T3 cells, however, reported excellent antibacterial properties against *Staphylococcus aureus* and *Escherichia coli* with antibacterial rates approaching 100%.

Another important approach is producing highly porous alloy to facilitate the ingrowth of bone tissue through the pores, leading firm fixation, allowing the transportation of body fluid into implant acting a living prosthesis, and to reduce the Young's modulus [267, 268]. Several processing methods have been used such as powder metallurgy with space-holder technique, microwave sintering, polymeric sponge process, gel-casting, and selective laser melting (SLM) to produce porous β-Ti Ti–Nb and Ti–Mo based alloys [269–273]. Furthermore, several morphologies of HA was electrochemically deposited on porous low Young's modulus Ti–40Nb alloy by various electrolytes and treatment times [270].

3 Discussion

Particularly during the last decade, β-Ti alloys have been extensively developed to reduce the high Young's modulus of cp-Ti and Ti–6Al–4V alloy. Although the developed β-Ti alloys still have higher Young's modulus compared to bone, the values close to 45 GPa reported for several alloys by adjusting the amount and type of β stabilizer alloying elements [274–277]. Similar to cp-Ti and Ti–6Al–4V, β-Ti alloys are bioinert materials, thus require surface modifications to obtain bioactivity. Furthermore, lower corrosion, wear, and tribocorrosion behaviour of β-Ti alloys have been recently reported compared to Ti–6Al–4V alloy, which are other crucial factors for long-term implants [58, 86, 278–280].

Mechanical treatments are being performed to form a nanocrystalline surface layer and grain refinement to improve the surface roughness and hardness or to alter the surface topography to gain bio-functions [281]. The mechanical, corrosion, wear, and biological behaviour of β-Ti alloys have been improved by HPT, SMAT, UNSM, and ARB severe plastic deformation techniques mainly due to the grain refinement from coarse grains to ultrafine grains. The ultrafine-grained Ti alloys prepared by severe plastic deformation are reported to have higher strength and cell bioactivity than the untreated ones [68]. However, tribocorrosion behaviour of severe plastic deformed β-Ti alloys are, to the best of our knowledge, yet to be studied.

Physical surface treatments of β-Ti alloys including PVD, plasma spraying, plasma nitriding, gas nitriding, and ion implantation treatments have been widely used to improve the corrosion and wear behaviour along with the bioactivity of metallic materials. Although physical surface treatments can improve the wear resistance of β-Ti alloys to some extent, physical deposition methods mostly require complex equipment and the resulting surfaces prone to delaminate under sliding conditions [95].

Chemical and electrochemical methods, allowing the incorporation of bioactive elements and providing stronger adhesion between bones and implant surfaces compared to the materials treated by mechanical and physical methods,

are attracting more attention owing to their lower cost and easier process control. These surface treatments can be used to generate a nanopatterned surface topography which is expected to be promising for the stimulation of bone tissue growth (osteointegration of bone tissue) [176]. One of the most used methods for bio-functionalization of β-Ti alloys is MAO treatment. As described previously, the MAO-layers on β-Ti alloys are characterized in terms of biological response by in vitro and in vivo studies. However, studies on the corrosion behaviour of these layers is still scarce and there is still lack of information regarding their corrosion mechanisms mainly, particularly the role of oxides of β stabilizer alloying elements, which may change the chemistry, structure and mechanical properties of MAO layer. Moreover, the corrosion behaviour should also be studied under conditions closer to in vivo, for instance, in a dynamic electrolyte and/or under the presence of proteins, enzymes, microorganisms, and biofilms. After implantation, micromovements occur between the implant and the hosting bone, or between the parts of the prosthesis, thus, understanding the effect of the combined action of corrosion and wear (tribocorrosion) is extremely important. Furthermore, the combined actions of corrosion and mechanical solicitations (fatigue-corrosion) also needs to be studied.

The nanotubular layer formation on β-Ti alloys is another common surface functionalization method. The nanotubular layer formation on the new alloys and its corrosion behaviour has been studied in the literature, however, the wear and tribocorrosion behaviour of these nanotubular layers are scarcely researched. The nanotubular layer grown on Ti has significantly poor adhesion to the substrate. Although some efforts are given in the literature [282–289], adhesion is still a major limitation for different applications [283, 290, 291]. To our best knowledge, there is no published study yet that investigates the tribocorrosion behaviour of nanotubular layer formed on β-Ti alloys, but the dry sliding behaviour of nanotubular layer formed on Ti–35Nb are reported, where the nanotubular layer improved the tribological behaviour of Ti–35Nb alloy even though this improvement was due to the tribolayer formed after smashing of the nanotubular layer during sliding [292].

Laser surface treatment is becoming one of the most efficient and versatile surface modification techniques, allowing to control changes in the mechanical, chemical, and physical properties of the surface through direct interaction of beam and substrate [293]. Laser treatment is being used to modify the substrate surfaces like texturing, hardening, remelting, and cladding, which can also be used to add calcium phosphate or HA. Based on the published studies, it can be stated that laser surface treatments are beneficial pre-treatments for the adhesion of nanotubes and bio-ceramic coatings, also they make a positive influence on corrosion, wear, and bioactivity of β-Ti alloys. However, laser texture and remelting may cause cracks on the surface, and the heat affected zone under the melting layer may lead to poor mechanical integrity. Also, in vitro and in vivo biological behaviour of laser-treated substrates are yet to be completely understood.

Recently, hybrid/multi-layered treatments have been attracted attention as a route to multifunctional materials. Depending on the target implant application, the surface of β-Ti alloys can be tailored by hybrid treatments. So far, HA/Nanotubes and HA/MAO has been the most studied hybrid treatments mainly to improve the adhesion of the HA layer through mechanical interlocking. Also, TiN coating on nanotubes has been studied to improve the wear resistance [227]. However, as discussed above, the main concern with nanotubular layers is the poor adhesion strength of nanotubes to the substrate. Thus, if a sufficient adhesion is not obtained between the substrate and the nanotubular layer, detached hard TiN particles may lead to catastrophic wear by acting as extra abrasives during relative movements. Therefore, even though each treatment has promising behaviour, individually, overall mechanical and triboelectrochemical responses of the hybrid/multi-layered surfaces need to be explored.

4 Concluding Remarks

β-Ti alloys show high durability, high toughness, non-toxicity, and high strength, which are specific advantages against other biomaterials. However, β-Ti alloys are typical artificial materials having bioinert behaviour. Therefore, the surface of a β-Ti alloy needs modification to improve the wear resistance and bioactive properties. In this review, an overview was given on the surface bio-functionalization methods applied to β-Ti alloys. Mechanical, physical, chemical, electrochemical methods, and immobilization of bio-functional molecules were discussed. The bioactivity, biocompatibility, haemocompatibility, wear and corrosion (tribocorrosion) resistance of β-Ti alloys can be improved by surface modification with desired properties, altering the surface composition or removing the undesired material from the alloy surface. Mainly, the bio-functionalization of β-Ti alloys include increasing the surface roughness and incorporating bioactive agents (Ca, P, Sr, Ag, Zn) or coating with HA and biomolecules. Undoubtedly, the ongoing work in this area will bring new materials and new techniques to enhance the quality of implant materials, which eventually can improve the quality of patient lifestyle.

Acknowledgements This work was supported by FCT national funds, under the national support to R&D units grant, through the reference project UIDB/04436/2020 and UIDP/04436/2020, together with M-ERA-NET/0001/2015 project. I. Çaha is grateful for financial support through PhD grant under the NORTE-08-5369-FSE-000012 project.

Compliance with Ethical Standards

Conflict of interest The authors declare that they have no known competing financial interests or personal relationships that could have appeared to influence the work reported in this paper.

References

1. Mihov D, Katerska B (2010) Some biocompatible materials used in medical practice. Trakia J Sci 8:119–125. https://doi.org/10.2320/matertrans.L-MRA2008828
2. Pandey E, Srivastava K, Gupta S, Srivastava S, Mishra N (2016) Some biocompatible materials used in medical practices—a review. Int J Pharm Sci Res 7:2748–2755
3. Niinomi M (2002) Recent metallic materials for biomedical applications. Metall Mater Trans A 33:477–486. https://doi.org/10.1007/s11661-002-0109-2
4. Niinomi M (2008) Mechanical biocompatibilities of titanium alloys for biomedical applications. J Mech Behav Biomed Mater 1:30–42. https://doi.org/10.1016/j.jmbbm.2007.07.001
5. Geetha M, Singh AK, Asokamani R, Gogia AK (2009) Ti based biomaterials, the ultimate choice for orthopaedic implants—A review. Prog Mater Sci 54:397–425. https://doi.org/10.1016/j.pmatsci.2008.06.004
6. Correa DRN, Vicente FB, Donato TAG, Arana-Chavez VE, Buzalaf MAR, Grandini CR (2014) The effect of the solute on the structure, selected mechanical properties, and biocompatibility of Ti–Zr system alloys for dental applications. Mater Sci Eng C 34:354–359. https://doi.org/10.1016/j.msec.2013.09.032
7. Kirmanidou Y, Sidira M, Drosou M-E, Bennani V, Bakopoulou A, Tsouknidas A, Michailidis N, Michalakis K (2016) New Ti-alloys and surface modifications to improve the mechanical properties and the biological response to orthopedic and dental implants: a review. Biomed Res Int 2016:1–21. https://doi.org/10.1155/2016/2908570
8. Okazaki Y (2001) A new Ti–15Zr–4Nb–4Ta alloy for medical applications. Curr Opin Solid State Mater Sci 5:45–53. https://doi.org/10.1016/S1359-0286(00)00025-5
9. Godley R, Starosvetsky D, Gotman I (2006) Corrosion behavior of a low modulus β-Ti-45 % Nb alloy for use in medical implants. J Mater Sci Med 17:63–67. https://doi.org/10.1007/s10856-006-6330-6
10. Perl DP (1985) Relationship of aluminum to Alzheimer's disease. Environ Health Perspect 63:149–153. https://doi.org/10.1289/ehp.8563149
11. Boyer R, Welsch G (1994) Materials properties handbook: titanium alloys. ASM International, Materials Park, OH
12. Niinomi M (1998) Mechanical properties of biomedical titanium alloys. Mater Sci Eng A 243:231–236. https://doi.org/10.1016/S0921-5093(97)00806-X
13. Department of Health and Human Services (2008) Public health statement for aluminum, agency toxic substances and disease registry 9. https://www.atsdr.cdc.gov/phs/phs.asp?id=1076&tid=34
14. Kuroda D, Niinomi M, Morinaga M, Kato Y, Yashiro T (1998) Design and mechanical properties of new β type titanium alloys for implant materials. Mater Sci Eng A 243(243):244–249. https://doi.org/10.1016/S0921-5093(97)00808-3
15. Long M, Rack HJ (1998) Titanium alloys in total joint replacement—a materials science perspective. Biomaterials 19:1621–1639. https://doi.org/10.1016/S0142-9612(97)00146-4
16. Niinomi M (2003) Fatigue performance and cyto-toxicity of low rigidity titanium alloy, Ti–29Nb–13Ta–4.6Zr. Biomaterials 24:2673–2683. https://doi.org/10.1016/S0142-9612(03)00069-3
17. Evans FG (1976) Mechanical properties and histology of cortical bone from younger and older men. Anat Rec 185:1–11. https://doi.org/10.1002/ar.1091850102
18. Brunette DM, Tengvall P, Textor M, Thomsen P (2001) Material science, surface science, engineering, biological responses and medical applications. Titanium in medicine, vol 49. Springer, Berlin, p 69126. https://doi.org/10.1007/978-3-642-56486-4
19. Ho WF, Ju CP, Chern Lin JH (1999) Structure and properties of cast binary Ti–Mo alloys. Biomaterials 20:2115–2122. https://doi.org/10.1016/S0142-9612(99)00114-3
20. Raabe D, Sander B, Friák M, Ma D, Neugebauer J (2007) Theory-guided bottom-up design of β-titanium alloys as biomaterials based on first principles calculations: theory and experiments. Acta Mater 55:4475–4487. https://doi.org/10.1016/j.actamat.2007.04.024
21. Cimpean A, Mitran V, Ciofrangeanu CM, Galateanu B, Bertrand E, Gordin DM, Iordachescu D, Gloriant T (2012) Osteoblast cell behavior on the new beta-type Ti–25Ta–25Nb alloy. Mater Sci Eng C 32:1554–1563. https://doi.org/10.1016/j.msec.2012.04.042
22. Ikeda M, Komatsu S-Y, Sowa I, Niinomi M (2002) Aging behavior of the Ti–29Nb–13Ta–4.6Zr new beta alloy for medical implants. Metall Mater Trans A 33:487–493. https://doi.org/10.1007/s11661-002-0110-9
23. Niinomi M, Hattori T, Morikawa K, Kasuga T, Suzuki A, Fukui H, Niwa S (2002) Development of low rigidity β-type titanium alloy for biomedical applications. Mater Trans 43:2970–2977. https://doi.org/10.2320/matertrans.43.2970
24. Gordin DM, Gloriant T, Nemtoi G, Chelariu R, Aelenei N, Guillou A, Ansel D (2005) Synthesis, structure and electrochemical behavior of a beta Ti–12Mo–5Ta alloy as new biomaterial. Mater Lett 59:2959–2964. https://doi.org/10.1016/j.matlet.2004.09.064
25. Qazi JI, Rack HJ (2005) Metastable beta titanium alloys for orthopedic applications. Adv Eng Mater 7:993–998. https://doi.org/10.1002/adem.200500060
26. Banerjee R, Nag S, Fraser H (2005) A novel combinatorial approach to the development of beta titanium alloys for orthopaedic implants. Mater Sci Eng C 25:282–289. https://doi.org/10.1016/j.msec.2004.12.010
27. Nag S, Banerjee R, Fraser HL (2005) Microstructural evolution and strengthening mechanisms in Ti–Nb–Zr–Ta, Ti–Mo–Zr–Fe and Ti–15Mo biocompatible alloys. Mater Sci Eng C. https://doi.org/10.1016/j.msec.2004.12.013
28. Elias LM, Schneider SG, Schneider S, Silva HM, Malvisi F (2006) Microstructural and mechanical characterization of biomedical Ti–Nb–Zr(–Ta) alloys. Mater Sci Eng A 432:108–112. https://doi.org/10.1016/j.msea.2006.06.013
29. Gloriant T, Texier G, Prima F, Laillé D, Gordin DM, Thibon I, Ansel D (2006) Synthesis and phase transformations of beta metastable Ti-based alloys containing biocompatible Ta, Mo and Fe beta-stabilizer elements. Adv Eng Mater 8:961–965. https://doi.org/10.1002/adem.200600106
30. Abdel-Hady M, Hinoshita K, Morinaga M (2006) General approach to phase stability and elastic properties of β-type Ti-alloys using electronic parameters. Scr Mater 55:477–480. https://doi.org/10.1016/j.scriptamat.2006.04.022
31. Matsuno H, Yokoyama A, Watari F, Uo M, Kawasaki T (2001) Biocompatibility and osteogenesis of refractory metal implants, titanium, hafnium, niobium, tantalum and rhenium. Biomaterials 22:1253–1262. https://doi.org/10.1016/S0142-9612(00)00275-1
32. Eisenbarth E, Velten D, Müller M, Thull R, Breme J (2004) Biocompatibility of β-stabilizing elements of titanium alloys. Biomaterials 25:5705–5713. https://doi.org/10.1016/j.biomaterials.2004.01.021
33. Niinomi M (2007) Recent research and development in metallic materials for biomedical, dental and healthcare

products applications. In: THERMEC 2006. Trans Tech Publications, pp 193–200. https://doi.org/10.4028/www.scientific.net/MSF.539-543.193
34. More NS, Paul SN, Roy M (2018) Electrochemical corrosion behaviour of Ti–29Nb–13Ta–4.6Zr alloy in physiological solution containing various synovial joint lubricants. J. Bio Tribo Corros. https://doi.org/10.1007/s40735-018-0156-x
35. Çaha I, Alves A, Chirico C, Pinto A, Tsipas S, Gordo E, Toptan F (2020) Corrosion and tribocorrosion behavior of Ti–40Nb and Ti–25Nb–5Fe alloys processed by powder metallurgy. Metall Mater Trans A 51:3256–3267. https://doi.org/10.1007/s11661-020-05757-6
36. Niinomi M (2008) Biologically and mechanically biocompatible titanium alloys. Mater Trans 49:2170–2178. https://doi.org/10.2320/matertrans.L-MRA2008828
37. Niinomi M, Ogawa M, Kinoshita T, Ikeda M, Ueda M (2012) Influence of Fe content of Ti–Mn–Fe alloys on phase constitution and heat treatment behavior. In: THERMEC 2011. Trans Tech Publications, pp 1893–1898. https://doi.org/10.4028/www.scientific.net/MSF.706-709.1893
38. Hosoda H, Kyogoku H, Ashida S (2012) Fabrication of Ti–Sn–Cr shape memory alloy by PM process and its properties. In: THERMEC 2011. Trans Tech Publications, pp 1943–1947. https://doi.org/10.4028/www.scientific.net/MSF.706-709.1943
39. Griza S, de Souza Sá DHG, Batista WW, de Blas JCG, Pereira LC (2014) Microstructure and mechanical properties of hot rolled TiNbSn alloys. Mater Des 56:200–208. https://doi.org/10.1016/j.matdes.2013.10.067
40. Niinomi M, Liu Y, Nakai M, Liu H, Li H (2016) Biomedical titanium alloys with Young's moduli close to that of cortical bone. Regen Biomater 3:173–185. https://doi.org/10.1093/rb/rbw016
41. Akahori T, Niinomi M, Fukui H, Ogawa M, Toda H (2005) Improvement in fatigue characteristics of newly developed beta type titanium alloy for biomedical applications by thermo-mechanical treatments. Mater Sci Eng C. https://doi.org/10.1016/j.msec.2004.12.007
42. Wang G, Hui S, Ye W, Mi X, Wang Y, Zhang W (2012) Microstructure and tensile properties of low cost titanium alloys at different cooling rate. Rare Met 31:531–536. https://doi.org/10.1007/s12598-012-0552-1
43. Yilmazer H, Niinomi M, Nakai M, Hieda J, Todaka Y, Akahori T, Miyazaki T (2012) Heterogeneous structure and mechanical hardness of biomedical β-type Ti–29Nb–13Ta–4.6Zr subjected to high-pressure torsion. J Mech Behav Biomed Mater 10:235–245. https://doi.org/10.1016/j.jmbbm.2012.02.022
44. Yilmazer H, Niinomi M, Nakai M, Cho K, Hieda J, Todaka Y, Miyazaki T (2013) Mechanical properties of a medical β-type titanium alloy with specific microstructural evolution through high-pressure torsion. Mater Sci Eng C 33:2499–2507. https://doi.org/10.1016/j.msec.2013.01.056
45. Tian Y, Yu Z, Ong CYA, Kent D, Wang G (2015) Microstructure, elastic deformation behavior and mechanical properties of biomedical β-type titanium alloy thin-tube used for stents. J Mech Behav Biomed Mater 45:132–141. https://doi.org/10.1016/j.jmbbm.2015.02.001
46. Mohammed MT, Khan ZA, Geetha M, Siddiquee AN (2015) Microstructure, mechanical properties and electrochemical behavior of a novel biomedical titanium alloy subjected to thermo-mechanical processing including aging. J Alloys Compd 634:272–280. https://doi.org/10.1016/j.jallcom.2015.02.095
47. Li YY, Zou LM, Yang C, Li YH, Li LJ (2013) Ultrafine-grained Ti-based composites with high strength and low modulus fabricated by spark plasma sintering. Mater Sci Eng A 560:857–861. https://doi.org/10.1016/j.msea.2012.09.047
48. Datta S, Mahfouf M, Zhang Q, Chattopadhyay PP, Sultana N (2016) Imprecise knowledge based design and development of titanium alloys for prosthetic applications. J Mech Behav Biomed Mater 53:350–365. https://doi.org/10.1016/j.jmbbm.2015.08.039
49. Geng F, Niinomi M, Nakai M (2011) Observation of yielding and strain hardening in a titanium alloy having high oxygen content. Mater Sci Eng A 528:5435–5445. https://doi.org/10.1016/j.msea.2011.03.064
50. Niinomi M, Nakai M (2012) Unusual effect of oxygen on the mechanical behavior of a β-type titanium alloy developed for biomedical applications. Mater Sci Forum 706–709:135–142. https://doi.org/10.4028/www.scientific.net/MSF.706-709.135
51. Manivasagam G, Dhinasekaran D, Rajamanickam A (2010) Biomedical implants: corrosion and its prevention—a review, recent patents. Corros Sci 2:40–54. https://doi.org/10.2174/1877610801002010040
52. Han MK, Kim JY, Hwang MJ, Song HJ, Park YJ (2015) Effect of Nb on the microstructure, mechanical properties, corrosion behavior, and cytotoxicity of Ti–Nb alloys. Materials (Basel) 8:5986–6003. https://doi.org/10.3390/ma8095287
53. Bai Y, Deng Y, Zheng Y, Li Y, Zhang R, Lv Y, Zhao Q, Wei S (2016) Characterization, corrosion behavior, cellular response and in vivo bone tissue compatibility of titanium–niobium alloy with low Young's modulus. Mater Sci Eng C 59:565–576. https://doi.org/10.1016/j.msec.2015.10.062
54. Bai YJ, Wang YB, Cheng Y, Deng F, Zheng YF, Wei SC (2011) Comparative study on the corrosion behavior of Ti–Nb and TMA alloys for dental application in various artificial solutions. Mater Sci Eng C 31:702–711. https://doi.org/10.1016/j.msec.2010.12.010
55. Biesiekierski A, Ping DH, Yamabe-Mitarai Y, Wen C (2014) Impact of ruthenium on microstructure and corrosion behavior of β-type Ti–Nb–Ru alloys for biomedical applications. Mater Des 59:303–309. https://doi.org/10.1016/j.matdes.2014.02.058
56. Gebert A, Oswald S, Helth A, Voss A, Gostin PF, Rohnke M, Janek J, Calin M, Eckert J (2015) Effect of indium (In) on corrosion and passivity of a beta-type Ti–Nb alloy in Ringer's solution. Appl Surf Sci 335:213–222. https://doi.org/10.1016/j.apsusc.2015.02.058
57. Dalmau A, Guiñón Pina V, Devesa F, Amigó V, Igual Muñoz A (2015) Electrochemical behavior of near-beta titanium biomedical alloys in phosphate buffer saline solution. Mater Sci Eng C 48:56–62. https://doi.org/10.1016/j.msec.2014.11.036
58. Çaha I, Alves AC, Kuroda PAB, Grandini CR, Pinto AMP, Rocha LA, Toptan F (2020) Degradation behavior of Ti–Nb alloys: corrosion behavior through 21 days of immersion and tribocorrosion behavior against alumina. Corros Sci 167:108488. https://doi.org/10.1016/j.corsci.2020.108488
59. Moraes PEL, Contieri RJ, Lopes ESN, Robin A, Caram R (2014) Effects of Sn addition on the microstructure, mechanical properties and corrosion behavior of Ti–Nb–Sn alloys. Mater Charact 96:273–281. https://doi.org/10.1016/j.matchar.2014.08.014
60. Atapour M, Pilchak AL, Frankel GS, Williams JC (2011) Corrosion behavior of β titanium alloys for biomedical applications. Mater Sci Eng C 31:885–891. https://doi.org/10.1016/j.msec.2011.02.005
61. Guo WY, Sun J, Wu JS (2009) Electrochemical and XPS studies of corrosion behavior of Ti–23Nb–0.7Ta–2Zr–O alloy in Ringer's solution. Mater Chem Phys 113:816–820. https://doi.org/10.1016/j.matchemphys.2008.08.043
62. Robin A, Carvalho OAS, Schneider SG, Schneider S (2008) Corrosion behavior of Ti–xNb–13Zr alloys in Ringer's solution. Mater Corros 59:929–933. https://doi.org/10.1002/maco.200805014
63. Málek J, Hnilica F, Veselý J, Smola B, Kolařík K, Fojt J, Vlach M, Kodetová V (2016) The effect of Zr on the microstructure and properties of Ti–35Nb–XZr alloy. Mater Sci Eng A 675:1–10. https://doi.org/10.1016/j.msea.2016.07.069

64. Ribeiro ALR, Hammer P, Vaz LG, Rocha LA (2013) Are new TiNbZr alloys potential substitutes of the Ti6Al4V alloy for dental applications? An electrochemical corrosion study. Biomed Mater. https://doi.org/10.1088/1748-6041/8/6/065005
65. Assis SL, Costa I (2007) Electrochemical evaluation of Ti–13Nb–13Zr, Ti–6Al–4V and Ti–6Al–7Nb alloys for biomedical application by long-term immersion tests. Mater Corros 58:329–333. https://doi.org/10.1002/maco.200604027
66. Yang S, Zhang DC, Wei M, Su HX, Wu W, Lin JG (2013) Effects of the Zr and Mo contents on the electrochemical corrosion behavior of Ti–22Nb alloy. Mater Corros 64:402–407. https://doi.org/10.1002/maco.201106478
67. Çaha I, Alves AC, Chirico C, Tsipas SA, Rodrigues IR, Pinto AMP, Grandini CR, Rocha LA, Gordo E, Toptan F (2020) Interactions between wear and corrosion on cast and sintered Ti–12Nb alloy in comparison with the commercial Ti–6Al–4V alloy. Corros Sci 176:108925. https://doi.org/10.1016/j.corsci.2020.108925
68. Zhang LC, Chen LY (2019) A review on biomedical titanium alloys: recent progress and prospect. Adv Eng Mater 21:1–29. https://doi.org/10.1002/adem.201801215
69. Liu X, Chen S, Tsoi JKH, Matinlinna JP (2017) Binary titanium alloys as dental implant materials—a review. Regen Biomater 4:315–323. https://doi.org/10.1093/rb/rbx027
70. Zhou YL, Luo DM (2011) Corrosion behavior of Ti–Mo alloys cold rolled and heat treated. J Alloys Compd 509:6267–6272. https://doi.org/10.1016/j.jallcom.2011.03.045
71. Oliveira NTC, Guastaldi AC (2008) Electrochemical behavior of Ti–Mo alloys applied as biomaterial. Corros Sci 50:938–945. https://doi.org/10.1016/j.corsci.2007.09.009
72. Oliveira NTC, Guastaldi AC (2009) Electrochemical stability and corrosion resistance of Ti–Mo alloys for biomedical applications. Acta Biomater 5:399–405. https://doi.org/10.1016/j.actbio.2008.07.010
73. Calderon Moreno JM, Vasilescu E, Drob P, Osiceanu P, Vasilescu C, Drob SI, Popa M (2013) Surface analysis and electrochemical behavior of Ti–20Zr alloy in simulated physiological fluids. Mater Sci Eng B 178:1195–1204. https://doi.org/10.1016/j.mseb.2013.07.006
74. Michelle Grandin H, Berner S, Dard M (2012) A review of titanium zirconium (TiZr) alloys for use in endosseous dental implants. Mater (Basel) 5:1348–1360. https://doi.org/10.3390/ma5081348
75. Akimoto T, Ueno T, Tsutsumi Y, Doi H, Hanawa T, Wakabayashi N (2018) Evaluation of corrosion resistance of implant-use Ti–Zr binary alloys with a range of compositions. J Biomed Mater Res B 106:73–79. https://doi.org/10.1002/jbm.b.33811
76. Zhou YL, Niinomi M, Akahori T, Fukui H, Toda H (2005) Corrosion resistance and biocompatibility of Ti–Ta alloys for biomedical applications. Mater Sci Eng A 398:28–36. https://doi.org/10.1016/j.msea.2005.03.032
77. Mareci D, Chelariu R, Gordin DM, Ungureanu G, Gloriant T (2009) Comparative corrosion study of Ti–Ta alloys for dental applications. Acta Biomater 5:3625–3639. https://doi.org/10.1016/j.actbio.2009.05.037
78. Ou SF, Wang CY (2017) Effects of bioceramic particles in dielectric of powder-mixed electrical discharge machining on machining and surface characteristics of titanium alloys. J Mater Process Technol 245:70–79. https://doi.org/10.1016/j.jmatprotec.2017.02.018
79. Manam NS, Harun WSW, Shri DNA, Ghani SAC, Kurniawan T, Ismail MH, Ibrahim MHI (2017) Study of corrosion in biocompatible metals for implants: a review. J Alloys Compd 701:698–715. https://doi.org/10.1016/j.jallcom.2017.01.196
80. Xue P, Li Y, Li K, Zhang D, Zhou C (2015) Superelasticity, corrosion resistance and biocompatibility of the Ti–19Zr–10Nb–1Fe alloy. Mater Sci Eng C 50:179–186. https://doi.org/10.1016/j.msec.2015.02.004
81. Nnamchi PS, Obayi CS, Todd I, Rainforth MW (2016) Mechanical and electrochemical characterisation of new Ti–Mo–Nb–Zr alloys for biomedical applications. J Mech Behav Biomed Mater 60:68–77. https://doi.org/10.1016/j.jmbbm.2015.12.023
82. Cordeiro JM, Beline T, Ribeiro ALR, Rangel EC, da Cruz NC, Landers R, Faverani LP, Vaz LG, Fais LMG, Vicente FB, Grandini CR, Mathew MT, Sukotjo C, Barão VAR (2017) Development of binary and ternary titanium alloys for dental implants. Dent Mater 33:1244–1257. https://doi.org/10.1016/j.dental.2017.07.013
83. Landolt D, Mischler S, Stemp M, Barril S (2004) Third body effects and material fluxes in tribocorrosion systems involving a sliding contact. Wear 256:517–524. https://doi.org/10.1016/S0043-1648(03)00561-1
84. Tian YS, Chen CZ, Chen LX, Huo QH (2006) Microstructures and wear properties of composite coatings produced by laser alloying of Ti–6Al–4V with graphite and silicon mixed powders. Mater Lett 60:109–113. https://doi.org/10.1016/j.matlet.2005.07.082
85. Fouvry S, Paulin C, Deyber S (2009) Impact of contact size and complex gross-partial slip conditions on Ti–6Al–4V/Ti–6Al–4V fretting wear. Tribol Int 42:461–474. https://doi.org/10.1016/j.triboint.2008.08.005
86. Cvijović-Alagić I, Cvijović Z, Mitrović S, Panić V, Rakin M (2011) Wear and corrosion behaviour of Ti–13Nb–13Zr and Ti–6Al–4V alloys in simulated physiological solution. Corros Sci 53:796–808. https://doi.org/10.1016/j.corsci.2010.11.014
87. Correa DRN, Kuroda PAB, Grandini CR, Rocha LA, Oliveira FGM, Alves AC, Toptan F (2016) Tribocorrosion behavior of β-type Ti–15Zr-based alloys. Mater Lett 179:118–121. https://doi.org/10.1016/j.matlet.2016.05.045
88. More NS, Diomidis N, Paul SN, Roy M, Mischler S (2011) Tribocorrosion behavior of β titanium alloys in physiological solutions containing synovial components. Mater Sci Eng C 31:400–408. https://doi.org/10.1016/j.msec.2010.10.021
89. Pina VG, Dalmau A, Devesa F, Amigó V, Muñoz AI (2015) Tribocorrosion behavior of beta titanium biomedical alloys in phosphate buffer saline solution. J Mech Behav Biomed Mater 46:59–68. https://doi.org/10.1016/j.jmbbm.2015.02.016
90. Narayanan R, Seshadri SK (2007) Phosphoric acid anodization of Ti–6Al–4V—structural and corrosion aspects. Corros Sci 49:542–558. https://doi.org/10.1016/j.corsci.2006.06.021
91. Deligianni DD, Katsala N, Ladas S, Sotiropoulou D, Amedee J, Missirlis YF (2001) Effect of surface roughness of the titanium alloy Ti–6Al–4V on human bone marrow cell response and on protein adsorption. Biomaterials 22:1241–1251. https://doi.org/10.1016/S0142-9612(00)00274-X
92. Gostin PF, Helth A, Voss A, Sueptitz R, Calin M, Eckert J, Gebert A (2013) Surface treatment, corrosion behavior, and apatite-forming ability of Ti–45Nb implant alloy. J Biomed Mater Res B 101(B):269–278. https://doi.org/10.1002/jbm.b.32836
93. Zareidoost A, Yousefpour M, Ghaseme B, Amanzadeh A (2012) The relationship of surface roughness and cell response of chemical surface modification of titanium. J Mater Sci Mater Med 23:1479–1488. https://doi.org/10.1007/s10856-012-4611-9
94. Lorenzetti M, Dogša I, Stošicki T, Stopar D, Kalin M, Kobe S, Novak S (2015) The influence of surface modification on bacterial adhesion to titanium-based substrates. ACS Appl Mater Interfaces 7:1644–1651. https://doi.org/10.1021/am507148n
95. Sasikumar Y, Indira K, Rajendran N (2019) Surface modification methods for titanium and its alloys and their corrosion behavior in biological environment: a review. J Bio Tribo Corros. https://doi.org/10.1007/s40735-019-0229-5

96. Ponsonnet L, Reybier K, Jaffrezic N, Comte V, Lagneau C, Lissac M, Martelet C (2003) Relationship between surface properties (roughness, wettability) of titanium and titanium alloys and cell behaviour. Mater Sci Eng C 23:551–560. https://doi.org/10.1016/S0928-4931(03)00033-X
97. Hoseini M, Jedenmalm A, Boldizar A (2008) Tribological investigation of coatings for artificial joints. Wear 264:958–966. https://doi.org/10.1016/j.wear.2007.07.003
98. Jiang SW, Jiang B, Li Y, Li YR, Yin GF, Zheng CQ (2004) Friction and wear study of diamond-like carbon gradient coatings on Ti6Al4V substrate prepared by plasma source ion implant-ion beam enhanced deposition. Appl Surf Sci 236:285–291. https://doi.org/10.1016/j.apsusc.2004.04.032
99. Manhabosco TM, Muller IL (2009) Electrodeposition of diamond-like carbon (DLC) films on Ti. Appl Surf Sci 255:4082–4086. https://doi.org/10.1016/j.apsusc.2008.10.087
100. Ma T, Chen T, Li WY, Wang S, Yang S (2011) Formation mechanism of linear friction welded Ti–6Al–4V alloy joint based on microstructure observation. Mater Charact 62:130–135. https://doi.org/10.1016/j.matchar.2010.11.009
101. Çaha I, Alves AC, Affonço LJ, Lisboa-Filho PN, da Silva JHD, Rocha LA, Pinto AMP, Toptan F (2019) Corrosion and tribocorrosion behaviour of titanium nitride thin films grown on titanium under different deposition times. Surf Coat Technol 374:878–888. https://doi.org/10.1016/j.surfcoat.2019.06.073
102. Xu J, Hu W, Xie ZH, Munroe P (2016) Reactive-sputter-deposited β-Ta_2O_5 and TaON nanoceramic coatings on Ti–6Al–4V alloy against wear and corrosion damage. Surf Coat Technol 296:171–184. https://doi.org/10.1016/j.surfcoat.2016.04.004
103. Ribeiro AM, Alves AC, Rocha LA, Silva FS, Toptan F (2014) Synergism between corrosion and wear on CoCrMo–Al_2O_3 biocomposites in a physiological solution. Tribol Int. https://doi.org/10.1016/j.triboint.2015.01.018
104. Toptan F, Rego A, Alves AC, Guedes A (2016) Corrosion and tribocorrosion behavior of Ti-B4C composite intended for orthopaedic implants. J Mech Behav Biomed Mater 61:152–163. https://doi.org/10.1016/j.jmbbm.2016.01.024
105. Silva JI, Alves AC, Pinto AM, Silva FS, Toptan F (2016) Dry sliding wear behaviour of Ti–TiB–TiNx in-situ composite synthesised by reactive hot pressing. Int J Surf Sci Eng 10:317–329. https://doi.org/10.1504/IJSURFSE.2016.077533
106. Silva JI, Alves AC, Pinto AM, Toptan F (2017) Corrosion and tribocorrosion behavior of Ti−TiB−TiNx in-situ hybrid composite synthesized by reactive hot pressing. J Mech Behav Biomed Mater 74:195–203. https://doi.org/10.1016/j.jmbbm.2017.05.041
107. Doni Z, Alves AC, Toptan F, Pinto AM, Rocha LA, Buciumeanu M, Palaghian L, Silva FS (2014) Tribocorrosion behaviour of hot pressed CoCrMo–Al_2O_3 composites for biomedical applications. Tribol Mater Surf Interfaces 8:201–208. https://doi.org/10.1179/1751584X14Y.0000000078
108. Doni Z, Alves AC, Toptan F, Rocha LA, Buciumeanu M, Palaghian L, Silva FS (2014) Tribocorrosion behaviour of hot pressed CoCrMo-HAP biocomposites. Tribol Int 91:221–227. https://doi.org/10.1016/j.triboint.2015.04.009
109. Gordo E, das Neves RG, Ferrari B, Jiménez-Morales A, Lima A, Alves AC, Pinto AM, Toptan F (2016) Corrosion and tribocorrosion behavior of Ti–alumina composites. Key Eng Mater 704:28–37. https://doi.org/10.4028/www.scientific.net/KEM.704.28
110. Alves SA, Patel SB, Sukotjo C, Mathew MT, Filho PN, Celis JP, Rocha LA, Shokuhfar T (2017) Synthesis of calcium-phosphorous doped TiO_2 nanotubes by anodization and reverse polarization: a promising strategy for an efficient biofunctional implant surface. Appl Surf Sci 399:682–701. https://doi.org/10.1016/j.apsusc.2016.12.105
111. Rodrigues NR, Alves AC, Toptan F, Rocha LA (2018) Preliminary investigation on the tribocorrosion behaviour of nanotubular structured Ti6Al4V surfaces. Mater Lett 213:214–217. https://doi.org/10.1016/j.matlet.2017.11.067
112. Sarraf M, Zalnezhad E, Bushroa AR, Hamouda AMS, Rafieerad AR, Nasiri-Tabrizi B (2015) Effect of microstructural evolution on wettability and tribological behavior of TiO_2 nanotubular arrays coated on Ti–6Al–4V. Ceram Int 41:7952–7962. https://doi.org/10.1016/j.ceramint.2015.02.136
113. Zalnezhad E, Baradaran S, Bushroa AR, Sarhan AAD (2014) Mechanical property enhancement of Ti–6Al–4V by multilayer thin solid film Ti/TiO_2 nanotubular array coating for biomedical application. Metall Mater Trans A 45:785–797. https://doi.org/10.1007/s11661-013-2043-x
114. Awad NK, Edwards SL, Morsi YS (2017) A review of TiO_2 NTs on Ti metal: electrochemical synthesis, functionalization and potential use as bone implants. Mater Sci Eng C 76:1401–1412. https://doi.org/10.1016/j.msec.2017.02.150
115. Mansoorianfar M, Tavoosi M, Mozafarinia R, Ghasemi A, Doostmohammadi A (2017) Preparation and characterization of TiO_2 nanotube arrays on Ti6Al4V surface for enhancement of cell treatment. Surf Coat Technol 321:409–415. https://doi.org/10.1016/j.surfcoat.2017.05.016
116. Taubert A, Mano JF, Rodríguez-Cabello JC (2013) Biomaterials surface science. Wiley-VCH Verlag GmbH & Co. KGaA, Weinheim. https://doi.org/10.1002/9783527649600
117. Su Y, Luo C, Zhang Z, Hermawan H, Zhu D, Huang J, Liang Y, Li G, Ren L (2018) Bioinspired surface functionalization of metallic biomaterials. J Mech Behav Biomed Mater 77:90–105. https://doi.org/10.1016/j.jmbbm.2017.08.035
118. Prakash C, Kansal HK, Pabla BS, Puri S, Aggarwal A (2016) Electric discharge machining—a potential choice for surface modification of metallic implants for orthopedic applications: a review. Proc Inst Mech Eng B 230:331–353. https://doi.org/10.1177/0954405415579113
119. Prakash C, Kansal HK, Pabla BS, Puri S (2015) Processing and characterization of novel biomimetic nanoporous bioceramic surface on β-Ti implant by powder mixed electric discharge machining. J Mater Eng Perform 24:3622–3633. https://doi.org/10.1007/s11665-015-1619-6
120. Prakash C, Kansal HK, Pabla BS, Puri S (2016) Multi-objective optimization of powder mixed electric discharge machining parameters for fabrication of biocompatible layer on β-Ti alloy using NSGA-II coupled with Taguchi based response surface methodology. J Mech Sci Technol 30:4195–4204. https://doi.org/10.1007/s12206-016-0831-0
121. Prakash C, Kansal HK, Pabla BS, Puri S (2017) Experimental investigations in powder mixed electric discharge machining of Ti–35Nb–7Ta–5Zrβ-titanium alloy. Mater Manuf Process 32:274–285. https://doi.org/10.1080/10426914.2016.1198018
122. Prakash C, Kansal HK, Pabla BS, Puri S (2017) On the influence of nanoporous layer fabricated by PMEDM on β-Ti implant: biological and computational evaluation of bone-implant interface. Mater Today Proc 4:2298–2307. https://doi.org/10.1016/j.matpr.2017.02.078
123. Prakash C, Uddin MS (2017) Surface modification of β-phase Ti implant by hydroaxyapatite mixed electric discharge machining to enhance the corrosion resistance and in-vitro bioactivity. Surf Coat Technol 326:134–145. https://doi.org/10.1016/j.surfcoat.2017.07.040
124. Azadmanjiri J, Berndt CC, Kapoor A, Wen C (2015) Development of surface nano-crystallization in alloys by surface mechanical attrition treatment (SMAT). Crit Rev Solid State Mater Sci 40:164–181. https://doi.org/10.1080/10408436.2014.978446
125. Yang X, Pan H, Zhang J, Gao H, Shu B, Gong Y, Zhu X (2019) Progress in mechanical properties of gradient structured metallic materials induced by surface mechanical attrition treatment.

Mater Trans 60:1543–1552. https://doi.org/10.2320/matertrans.MF201911
126. Bahl S, Aleti BT, Suwas S, Chatterjee K (2018) Surface nanostructuring of titanium imparts multifunctional properties for orthopedic and cardiovascular applications. Mater Des 144:169–181. https://doi.org/10.1016/j.matdes.2018.02.022
127. Jin L, Cui W, Song X, Zhou L (2015) The formation mechanisms of surface nanocrystallites in β-type biomedical TiNbZrFe alloy by surface mechanical attrition treatment. Appl Surf Sci 347:553–560. https://doi.org/10.1016/j.apsusc.2015.04.137
128. Acharya S, Panicker AG, Gopal V, Dabas SS, Manivasagam G, Suwas S, Chatterjee K (2020) Surface mechanical attrition treatment of low modulus Ti–Nb–Ta–O alloy for orthopedic applications. Mater Sci Eng C 110:110729. https://doi.org/10.1016/j.msec.2020.110729
129. Huang R, Han Y (2013) The effect of SMAT-induced grain refinement and dislocations on the corrosion behavior of Ti–25Nb–3Mo–3Zr–2Sn alloy. Mater Sci Eng C 33:2353–2359. https://doi.org/10.1016/j.msec.2013.01.068
130. Wang M, Fan Y (2018) Electrochemical corrosion property of nanostructure layer of Ti–5Al–2Sn–2Zr–4Mo–4Cr titanium alloy. Int J Adv Manuf Technol 96:1601–1606. https://doi.org/10.1007/s00170-017-0660-z
131. Huang R, Zhang L, Huang L, Zhu J (2019) Enhanced in-vitro osteoblastic functions on β-type titanium alloy using surface mechanical attrition treatment. Mater Sci Eng C 97:688–697. https://doi.org/10.1016/j.msec.2018.12.082
132. Ma C, Andani MT, Qin H, Moghaddam NS, Ibrahim H, Jahadakbar A, Amerinatanzi A, Ren Z, Zhang H, Doll GL, Dong Y, Elahinia M, Ye C (2017) Improving surface finish and wear resistance of additive manufactured nickel–titanium by ultrasonic nano-crystal surface modification. J Mater Process Technol 249:433–440. https://doi.org/10.1016/j.jmatprotec.2017.06.038
133. Kheradmandfard M, Kashani-Bozorg SF, Kim C-L, Hanzaki AZ, Pyoun Y-S, Kim J-H, Amanov A, Kim D-E (2017) Nanostructured β-type titanium alloy fabricated by ultrasonic nanocrystal surface modification. Ultrason Sonochem. https://doi.org/10.1016/j.ultsonch.2017.03.061
134. Kheradmandfard M, Kashani-Bozorg SF, Lee JS, Kim CL, Hanzaki AZ, Pyun YS, Cho SW, Amanov A, Kim DE (2018) Significant improvement in cell adhesion and wear resistance of biomedical β-type titanium alloy through ultrasonic nanocrystal surface modification. J Alloys Compd 762:941–949. https://doi.org/10.1016/j.jallcom.2018.05.088
135. Xu W, Wu X, Figueiredo RB, Stoica M, Calin M, Eckert J, Langdon TG, Xia K (2009) Nanocrystalline body-centred cubic beta-titanium alloy processed by high-pressure torsion. Int J Mater Res. https://doi.org/10.3139/146.110229
136. Xu W, Edwards DP, Wu X, Stoica M, Calin M, Kühn U, Eckert J, Xia K (2013) Promoting nano/ultrafine-duplex structure via accelerated α precipitation in a β-type titanium alloy severely deformed by high-pressure torsion. Scr Mater 68:67–70. https://doi.org/10.1016/j.scriptamat.2012.09.023
137. Yilmazer H, Niinomi M, Cho K, Nakai M, Hieda J, Sato S, Todaka Y (2014) Microstructural evolution of precipitation-hardened β-type titanium alloy through high-pressure torsion. Acta Mater 80:172–182. https://doi.org/10.1016/j.actamat.2014.07.041
138. Gatina S, Semenova I, Leuthold J, Valiev R (2015) Nanostructuring and phase transformations in the β-alloy Ti–15Mo during high-pressure torsion. Adv Eng Mater 17:1742–1747. https://doi.org/10.1002/adem.201500104
139. Delshadmanesh M, Khatibi G, Ghomsheh MZ, Lederer M, Zehetbauer M, Danninger H (2017) Influence of microstructure on fatigue of biocompatible β-phase Ti–45Nb. Mater Sci Eng A 706:83–94. https://doi.org/10.1016/j.msea.2017.08.098
140. Yilmazer H, Şen M, Niinomi M, Nakai M, Huihong L, Cho K, Todaka Y, Shiku H, Matsue T (2016) Developing biomedical nano-grained β-type titanium alloys using high pressure torsion for improved cell adherence. RSC Adv 6:7426–7430. https://doi.org/10.1039/C5RA23454A
141. Dimić I, Cvijović-Alagić I, Hohenwarter A, Pippan R, Kojić V, Bajat J, Rakin M (2018) Electrochemical and biocompatibility examinations of high-pressure torsion processed titanium and Ti–13Nb–13Zr alloy. J Biomed Mater Res B 106:1097–1107. https://doi.org/10.1002/jbm.b.33919
142. Sharman K, Bazarnik P, Brynk T, Gunay Bulutsuz A, Lewandowska M, Huang Y, Langdon TG (2015) Enhancement in mechanical properties of a β-titanium alloy by high-pressure torsion. J Mater Res Technol 4:79–83. https://doi.org/10.1016/j.jmrt.2014.10.010
143. Janeček M, Čížek J, Stráský J, Václavová K, Hruška P, Polyakova V, Gatina S, Semenova I (2014) Microstructure evolution in solution treated Ti15Mo alloy processed by high pressure torsion. Mater Charact 98:233–240. https://doi.org/10.1016/j.matchar.2014.10.024
144. Pérez DAG, Jorge Junior AM, Roche V, Lepretre JC, Afonso CRM, Travessa DN, Asato GH, Bolfarini C, Botta WJ (2020) Severe plastic deformation and different surface treatments on the biocompatible Ti13Nb13Zr and Ti35Nb7Zr5Ta alloys: microstructural and phase evolutions, mechanical properties, and bioactivity analysis. J Alloys Compd. https://doi.org/10.1016/j.jallcom.2019.152116
145. Dimić I, Cvijović-Alagić I, Völker B, Hohenwarter A, Pippan R, Veljović D, Rakin M, Bugarski B (2016) Microstructure and metallic ion release of pure titanium and Ti–13Nb–13Zr alloy processed by high pressure torsion. Mater Des 91:340–347. https://doi.org/10.1016/j.matdes.2015.11.088
146. Nocivin A, Raducanu D, Cinca I, Trisca-Rusu C, Butu M, Thibon I, Cojocaru VD (2015) X-ray diffraction study and texture evolution for a Ti–Nb–Ta biomedical alloy processed by accumulative roll bonding. J Mater Eng Perform 24:1587–1601. https://doi.org/10.1007/s11665-015-1414-4
147. Cinca I, Raducanu D, Nocivin A, Gordin DM, Cojocaru VD (2013) Formation of nano-sized grains in Ti–10Zr–5Nb–5Ta biomedical alloy processed by accumulative roll bonding (ARB). Kov Mater 51:165–172. https://doi.org/10.4149/km.2013.3.165
148. Raducanu D, Vasilescu E, Cojocaru VD, Cinca I, Drob P, Vasilescu C, Drob SI (2011) Mechanical and corrosion resistance of a new nanostructured Ti–Zr–Ta–Nb alloy. J Mech Behav Biomed Mater 4:1421–1430. https://doi.org/10.1016/j.jmbbm.2011.05.012
149. Raducanu D, Vasilescu C, Nocivin A, Drob SI, Cinca I, Gordin D, Marcu M, Cojocaru VD (2014) Promoting structural and anticorrosive performances via accumulative roll bonding to a Ti–Ta–Nb alloy. Int J Electrochem Sci 10:4346–4358
150. Kent D, Wang G, Yu Z, Ma X, Dargusch M (2011) Strength enhancement of a biomedical titanium alloy through a modified accumulative roll bonding technique. J Mech Behav Biomed Mater 4:405–416. https://doi.org/10.1016/j.jmbbm.2010.11.013
151. Kent D, Xiao WL, Wang G, Yu Z, Dargusch MS (2012) Thermal stability of an ultrafine grain β-Ti alloy. Mater Sci Eng A 556:582–587. https://doi.org/10.1016/j.msea.2012.07.030
152. Moore B, Asadi E, Lewis G (2017) Deposition methods for microstructured and nanostructured coatings on metallic bone implants: a review. Adv Mater Sci Eng. https://doi.org/10.1155/2017/5812907
153. Zhao G, Xia L, Wen G, Song L, Wang X, Wu K (2012) Microstructure and properties of plasma-sprayed bio-coatings on a low-modulus titanium alloy from milled HA/Ti powders. Surf Coat Technol 206:4711–4719. https://doi.org/10.1016/j.surfcoat.2011.08.033

154. Zhao GL, Wen G, Song Y, Wu K (2011) Near surface martensitic transformation and recrystallization in a Ti–24Nb–4Zr–7.9Sn alloy substrate after application of a HA coating by plasma spraying. Mater Sci Eng C 31:106–113. https://doi.org/10.1016/j.msec.2010.08.003
155. He YH, Zhang YQ, Jiang YH, Zhou R (2016) Microstructure evolution and enhanced bioactivity of Ti–Nb–Zr alloy by bioactive hydroxyapatite fabricated via spark plasma sintering. RSC Adv 6:100939–100953. https://doi.org/10.1039/C6RA22986G
156. Toptan F, Alves AC, Ferreira MA, da Silva Oliveira CI, Pinto AMP (2018) Effect of HAP decomposition on the corrosion behavior of Ti-HAP biocomposites. Mater Corros. https://doi.org/10.1002/maco.201810049
157. Kim WG, Choe HC (2011) Surface characteristics of hydroxyapatite/titanium composite layer on the Ti–35Ta–xZr surface by RF and DC sputtering. Thin Solid Films 519:7045–7049. https://doi.org/10.1016/j.tsf.2011.04.090
158. Sathish S, Geetha M, Aruna ST, Balaji N, Rajam KS, Asokamani R (2011) Studies on plasma sprayed bi-layered ceramic coating on bio-medical Ti–13Nb–13Zr alloy. Ceram Int 37:1333–1339. https://doi.org/10.1016/j.ceramint.2010.12.012
159. Sathish S, Geetha M, Aruna ST, Balaji N, Rajam KS, Asokamani R (2011) Sliding wear behavior of plasma sprayed nanoceramic coatings for biomedical applications. Wear 271:934–941. https://doi.org/10.1016/j.wear.2011.03.023
160. Bédouin Y, Gordin DM, Pellen-Mussi P, Pérez F, Tricot-Doleux S, Vasilescu C, Drob SI, Chauvel-Lebret D, Gloriant T (2019) Enhancement of the biocompatibility by surface nitriding of a low-modulus titanium alloy for dental implant applications. J Biomed Mater Res B 107:1483–1490. https://doi.org/10.1002/jbm.b.34240
161. Akita M, Uematsu Y, Kakiuchi T, Nakajima M, Bai Y, Tamada K (2015) Fatigue behavior of bulk β-type titanium alloy Ti–15Mo–5Zr–3Al annealed in high temperature nitrogen gas. Mater Sci Eng A 627:351–359. https://doi.org/10.1016/j.msea.2015.01.022
162. Mohan L, Raja MD, Uma TS, Rajendran N, Anandan C (2016) In-vitro biocompatibility studies of plasma-nitrided titanium alloy β-21S using fibroblast cells. J Mater Eng Perform 25:1508–1514. https://doi.org/10.1007/s11665-015-1860-z
163. Cassar G, Matthews A, Leyland A (2012) Triode plasma diffusion treatment of titanium alloys. Surf Coat Technol 212:20–31. https://doi.org/10.1016/j.surfcoat.2012.09.006
164. Tian W, Guo Y, Li X, Tang B, Fan A (2017) Friction and wear behavior of modified layer prepared on Ti–13Nb–13Zr alloy by magnetron sputtering and plasma nitriding. J Wuhan Univ Technol Mater Sci Ed 32:951–957. https://doi.org/10.1007/s11595-017-1695-6
165. Çomakli O (2020) Influence of CrN, TiAlN monolayers and TiAlN/CrN multilayer ceramic films on structural, mechanical and tribological behavior of β-type Ti45Nb alloys. Ceram Int 46:8185–8191. https://doi.org/10.1016/j.ceramint.2019.12.046
166. Krishnan V, Krishnan A, Remya R, Ravikumar KK, Nair SA, Shibli SMA, Varma HK, Sukumaran K, Kumar KJ (2011) Development and evaluation of two PVD-coated β-titanium orthodontic archwires for fluoride-induced corrosion protection. Acta Biomater 7:1913–1927. https://doi.org/10.1016/j.actbio.2010.11.026
167. Ion R, Bédouin Y, Gloriant T, Andruseac G, Gordin DM, Cimpean A (2019) In vitro study of human endothelial progenitor cells behaviour on nitrided Ni-free Ti–27Nb alloy. Prog Nat Sci Mater Int 29:466–471. https://doi.org/10.1016/j.pnsc.2019.08.001
168. Zhecheva A, Malinov S, Sha W (2006) Titanium alloys after surface gas nitriding. Surf Coat Technol 201:2467–2474. https://doi.org/10.1016/j.surfcoat.2006.04.019
169. Yang C, Liu J (2019) Intermittent vacuum gas nitriding of TB8 titanium alloy. Vacuum 163:52–58. https://doi.org/10.1016/j.vacuum.2018.11.059
170. Gordin DM, Thibon I, Guillou A, Cornen M, Gloriant T (2010) Microstructural characterization of nitrided beta Ti–Mo alloys at 1400 °C. Mater Charact 61:376–380. https://doi.org/10.1016/j.matchar.2009.12.010
171. Vlcak P, Fojt J, Weiss Z, Kopeček J, Perina V (2019) The effect of nitrogen saturation on the corrosion behaviour of Ti–35Nb–7Zr–5Ta beta titanium alloy nitrided by ion implantation. Surf Coat Technol 358:144–152. https://doi.org/10.1016/j.surfcoat.2018.11.004
172. Carquigny S, Takadoum J, Ivanescu S (2019) Comparative study of nitrogen implantation effect on mechanical and tribological properties of Ti–6Al–4V and Ti–10Zr–10Nb–5Ta alloys. EPJ Appl Phys 85:5–10. https://doi.org/10.1051/epjap/2019180149
173. Gordin DM, Busardo D, Cimpean A, Vasilescu C, Höche D, Drob SI, Mitran V, Cornen M, Gloriant T (2013) Design of a nitrogen-implanted titanium-based superelastic alloy with optimized properties for biomedical applications. Mater Sci Eng C 33:4173–4182. https://doi.org/10.1016/j.msec.2013.06.008
174. Mohan L, Anandan C (2013) Effect of gas composition on corrosion behavior and growth of apatite on plasma nitrided titanium alloy Beta-21S. Appl Surf Sci 268:288–296. https://doi.org/10.1016/j.apsusc.2012.12.080
175. Mohan L, Anandan C (2013) Wear and corrosion behavior of oxygen implanted biomedical titanium alloy Ti–13Nb–13Zr. Appl Surf Sci 282:281–290. https://doi.org/10.1016/j.apsusc.2013.05.120
176. Kokubo T, Yamaguchi S (2015) Bioactive titanate layers formed on titanium and its alloys by simple chemical and heat treatments. Open Biomed Eng J 9:29–41. https://doi.org/10.2174/1874120701509010029
177. Helth A, Gostin PF, Oswald S, Wendrock H, Wolff U, Hempel U, Arnhold S, Calin M, Eckert J, Gebert A (2014) Chemical nanoroughening of Ti40Nb surfaces and its effect on human mesenchymal stromal cell response. J Biomed Mater Res B 102:31–41. https://doi.org/10.1002/jbm.b.32976
178. Müller FA, Bottino MC, Müller L, Henriques VAR, Lohbauer U, Bressiani AHA, Bressiani JC (2008) In vitro apatite formation on chemically treated (P/M) Ti–13Nb–13Zr. Dent Mater 24:50–56. https://doi.org/10.1016/j.dental.2007.02.005
179. Yamaguchi S, Hashimoto H, Nakai R, Takadama H (2017) Impact of surface potential on apatite formation in Ti alloys subjected to acid and heat treatments. Materials (Basel). https://doi.org/10.3390/ma10101127
180. Schmidt R, Hoffmann V, Helth A, Gostin PF, Calin M, Eckert J, Gebert A (2016) Electrochemical deposition of hydroxyapatite on beta-Ti–40Nb. Surf Coat Technol 294:186–193. https://doi.org/10.1016/j.surfcoat.2016.03.063
181. Lee BH, Do Kim Y, Shin JH, Lee KH (2002) Surface modification by alkali and heat treatments in titanium alloys. J Biomed Mater Res 61:466–473. https://doi.org/10.1002/jbm.10190
182. Sasikumar Y, Karthega M, Rajendran N (2011) In vitro bioactivity of surface-modified β-Ti alloy for biomedical applications. J Mater Eng Perform 20:1271–1277. https://doi.org/10.1007/s11665-010-9772-4
183. Ban S (2003) Effect of alkaline treatment of pure titanium and its alloys on the bonding strength of dental veneering resins. J Biomed Mater Res A 66:138–145. https://doi.org/10.1002/jbm.a.10566
184. Takematsu E, Katsumata K, Okada K, Niinomi M, Matsushita N (2016) Bioactive surface modification of Ti–29Nb–13Ta–4.6Zr alloy through alkali solution treatments. Mater Sci Eng C 62:662–667. https://doi.org/10.1016/j.msec.2016.01.041

185. Sasikumar Y, Rajendran N (2013) Influence of surface modification on the apatite formation and corrosion behavior of Ti and Ti–15Mo alloy for biomedical applications. Mater Chem Phys 138:114–123. https://doi.org/10.1016/j.matchemphys.2012.11.025
186. Kumar AM, Sudhagar P, Ramakrishna S, Kang YS, Kim H, Gasem ZM, Rajendran N (2014) Evaluation of chemically modified Ti–5Mo–3Fe alloy surface: electrochemical aspects and in vitro bioactivity on MG63 cells. Appl Surf Sci 307:52–61. https://doi.org/10.1016/j.apsusc.2014.03.146
187. Shukla AK, Balasubramaniam R (2006) Effect of surface treatment on electrochemical behavior of CP Ti, Ti–6Al–4V and Ti–13Nb–13Zr alloys in simulated human body fluid. Corros Sci 48:1696–1720. https://doi.org/10.1016/j.corsci.2005.06.003
188. Li PF, Xu Y, Cheng XH (2013) Chemisorption of thermal reduced graphene oxide nano-layer film on TNTZ surface and its tribological behavior. Surf Coat Technol 232:331–339. https://doi.org/10.1016/j.surfcoat.2013.05.030
189. Zheng CY, Li SJ, Tao XJ, Hao YL, Yang R, Zhang L (2007) Calcium phosphate coating of Ti–Nb–Zr–Sn titanium alloy. Mater Sci Eng C 27:824–831. https://doi.org/10.1016/j.msec.2006.09.021
190. Takematsu E, Cho K, Hieda J, Nakai M, Katsumata K, Okada K, Niinomi M, Matsushita N (2016) Adhesive strength of bioactive oxide layers fabricated on TNTZ alloy by three different alkali-solution treatments. J Mech Behav Biomed Mater 61:174–181. https://doi.org/10.1016/j.jmbbm.2015.12.046
191. Takematsu E, Noguchi K, Kuroda K, Ikoma T, Niinomi M, Matsushita N (2018) In vivo osteoconductivity of surface modified Ti–29Nb–13Ta–4.6Zr alloy with low dissolution of toxic trace elements. PLoS ONE 13:1–12. https://doi.org/10.1371/journal.pone.0189967
192. Hieda J, Niinomi M, Nakai M, Cho K, Gozawa T, Katsui H, Tu R, Goto T (2013) Enhancement of adhesive strength of hydroxyapatite films on Ti–29Nb–13Ta–4.6Zr by surface morphology control. J Mech Behav Biomed Mater 18:232–239. https://doi.org/10.1016/j.jmbbm.2012.11.013
193. Zuldesmi M, Waki A, Kuroda K, Okido M (2015) Hydrothermal treatment of titanium alloys for the enhancement of osteoconductivity. Mater Sci Eng C 49:430–435. https://doi.org/10.1016/j.msec.2015.01.031
194. Liu XH, Wu L, Ai HJ, Han Y, Hu Y (2015) Cytocompatibility and early osseointegration of nanoTiO_2-modified Ti–24Nb–4Zr–7.9Sn surfaces. Mater Sci Eng C 48:256–262. https://doi.org/10.1016/j.msec.2014.12.011
195. Zheng CY, Li SJ, Tao XJ, Hao YL, Yang R (2009) Surface modification of Ti–Nb–Zr–Sn alloy by thermal and hydrothermal treatments. Mater Sci Eng C 29:1245–1251. https://doi.org/10.1016/j.msec.2008.10.008
196. Tao F, Wei S (2014) Hydrothermal surface modification of a low modulus Ti–Nb based alloy. Rare Met Mater Eng 43:291–295. https://doi.org/10.1016/S1875-5372(14)60061-8
197. Kazek-Kęsik A, Dercz G, Suchanek K, Kalemba-Rec I, Piotrowski J, Simka W (2015) Biofunctionalization of Ti–13Nb–13Zr alloy surface by plasma electrolytic oxidation. Part I. Surf Coat Technol 276:59–69. https://doi.org/10.1016/j.surfcoat.2015.06.034
198. Minagar S, Berndt CC, Wang J, Ivanova E, Wen C (2012) A review of the application of anodization for the fabrication of nanotubes on metal implant surfaces. Acta Biomater 8:2875–2888. https://doi.org/10.1016/j.actbio.2012.04.005
199. Rafieerad AR, Ashra MR, Mahmoodian R, Bushroa AR (2015) Surface characterization and corrosion behavior of calcium phosphate-base composite layer on titanium and its alloys via plasma electrolytic oxidation: a review paper. Mater Sci Eng C 57:397–413. https://doi.org/10.1016/j.msec.2015.07.058
200. Simka W, Krząkała A, Korotin DM, Zhidkov IS, Kurmaev EZ, Cholakh SO, Kuna K, Dercz G, Michalska J, Suchanek K, Gorewoda T (2013) Modification of a Ti–Mo alloy surface via plasma electrolytic oxidation in a solution containing calcium and phosphorus. Electrochim Acta 96:180–190. https://doi.org/10.1016/j.electacta.2013.02.102
201. Kazek-Kęsik A, Krok-Borkowicz M, Pamuła E, Simka W (2014) Electrochemical and biological characterization of coatings formed on Ti–15Mo alloy by plasma electrolytic oxidation. Mater Sci Eng C 43:172–181. https://doi.org/10.1016/j.msec.2014.07.021
202. Kazek-Kęsik A, Krok-Borkowicz M, Dercz G, Donesz-Sikorska A, Pamuła E, Simka W (2016) Multilayer coatings formed on titanium alloy surfaces by plasma electrolytic oxidation-electrophoretic deposition methods. Electrochim Acta 204:294–306. https://doi.org/10.1016/j.electacta.2016.02.193
203. Kazek-Kęsik A, Jaworska J, Krok-Borkowicz M, Gołda-Cępa M, Pastusiak M, Brzychczy-Włoch M, Pamuła E, Kotarba A, Simka W (2016) Hybrid oxide-polymer layer formed on Ti–15Mo alloy surface enhancing antibacterial and osseointegration functions. Surf Coat Technol 302:158–165. https://doi.org/10.1016/j.surfcoat.2016.05.073
204. Kazek-Kęsik A, Kuna K, Dec W, Widziołek M, Tylko G, Osyczka AM, Simka W (2016) In vitro bioactivity investigations of Ti–15Mo alloy after electrochemical surface modification. J Biomed Mater Res B 104:903–913. https://doi.org/10.1002/jbm.b.33442
205. Kazek-Kęsik A, Dercz G, Kalemba I, Suchanek K, Kukharenko AI, Korotin DM, Michalska J, Krząkała A, Piotrowski J, Kurmaev EZ, Cholakh SO, Simka W (2014) Surface characterisation of Ti–15Mo alloy modified by a PEO process in various suspensions. Mater Sci Eng C 39:259–272. https://doi.org/10.1016/j.msec.2014.03.008
206. Sowa M, Piotrowska M, Widziołek M, Dercz G, Tylko G, Gorewoda T, Osyczka AM, Simka W (2015) Bioactivity of coatings formed on Ti–13Nb–13Zr alloy using plasma electrolytic oxidation. Mater Sci Eng C 49:159–173. https://doi.org/10.1016/j.msec.2014.12.073
207. Sharkeev Y, Komarova E, Sedelnikova M, Sun ZM, Zhu QF, Zhang J, Tolkacheva T, Uvarkin P (2017) Structure and properties of micro-arc calcium phosphate coatings on pure titanium and Ti–40Nb alloy. Trans Nonferrous Met Soc China 27:125–133. https://doi.org/10.1016/S1003-6326(17)60014-1
208. Kazek-Kęsik A, Krok-Borkowicz M, Jakóbik-Kolon A, Pamuła E, Simka W (2015) Biofunctionalization of Ti–13Nb–13Zr alloy surface by plasma electrolytic oxidation. Part II. Surf Coat Technol 276:23–30. https://doi.org/10.1016/j.surfcoat.2015.06.035
209. Tao XJ, Li SJ, Zheng CY, Fu J, Guo Z, Hao YL, Yang R, Guo ZX (2009) Synthesis of a porous oxide layer on a multifunctional biomedical titanium by micro-arc oxidation. Mater Sci Eng C 29:1923–1934. https://doi.org/10.1016/j.msec.2009.03.004
210. Ou SF, Lin CS, Pan YN (2011) Microstructure and surface characteristics of hydroxyapatite coating on titanium and Ti–30Nb–1Fe–1Hf alloy by anodic oxidation and hydrothermal treatment. Surf Coat Technol 205:2899–2906. https://doi.org/10.1016/j.surfcoat.2010.10.063
211. Zhao L, Wei Y, Li J, Han Y, Ye R, Zhang Y (2010) Initial osteoblast functions on Ti–5Zr–3Sn–5Mo–15Nb titanium alloy surfaces modified by microarc oxidation. J Biomed Mater Res A 92:432–440. https://doi.org/10.1002/jbm.a.32348
212. Yu S, Yu ZT, Wang G, Han JY, Ma XQ, Dargusch MS (2011) Preparation and osteoinduction of active micro-arc oxidation films on Ti–3Zr–2Sn–3Mo–25Nb alloy. Trans Nonferrous Met Soc China 21:573–580. https://doi.org/10.1016/S1003-6326(11)60753-X

213. Gao Y, Gao B, Wang R, Wu J, Zhang LJ, Hao YL, Tao XJ (2009) Improved biological performance of low modulus Ti–24Nb–4Zr–7.9Sn implants due to surface modification by anodic oxidation. Appl Surf Sci 255:5009–5015. https://doi.org/10.1016/j.apsusc.2008.12.054
214. Pan YN, Lin CS, Wang KK, Ou SF (2014) Effect of Nb addition on anodic behavior of Ti alloy in electrolyte containing calcium and phosphorus. Surf Coat Technol 258:1016–1024. https://doi.org/10.1016/j.surfcoat.2014.07.037
215. Ou SF, Chou HH, Lin CS, Shih CJ, Wang KK, Pan YN (2012) Effects of anodic oxidation and hydrothermal treatment on surface characteristics and biocompatibility of Ti–30Nb–1Fe–1Hf alloy. Appl Surf Sci 258:6190–6198. https://doi.org/10.1016/j.apsusc.2012.02.109
216. Correa DRN, Rocha LA, Ribeiro AR, Gemini-Piperni S, Archanjo BS, Achete CA, Werckmann J, Afonso CRM, Shimabukuro M, Doi H, Tsutsumi Y, Hanawa T (2018) Growth mechanisms of Ca- and P-rich MAO films in Ti–15Zr–xMo alloys for osseointegrative implants. Surf Coat Technol 344:373–382. https://doi.org/10.1016/j.surfcoat.2018.02.099
217. Chen H-T, Chung C-J, Yang T-C, Chiang I-P, Tang C-H, Chen K-C, He J-L (2010) Osteoblast growth behavior on micro-arc oxidized β-titanium alloy. Surf Coat Technol 205:1624–1629. https://doi.org/10.1016/j.surfcoat.2010.07.027
218. He X, Zhang X, Wang X, Qin L (2017) Review of antibacterial activity of titanium-based implants' surfaces fabricated by micro-arc oxidation. Coatings 7:45. https://doi.org/10.3390/coatings7030045
219. Kazek-Kesik A, Krok-Borkowicz M, Jakóbik-Kolon A, Pamuła E, Simka W (2015) Biofunctionalization of Ti–13Nb–13Zr alloy surface by plasma electrolytic oxidation. Part II. Surf Coat Technol 276:23–30. https://doi.org/10.1016/j.surfcoat.2015.06.035
220. Gebert A, Eigel D, Gostin PF, Hoffmann V, Uhlemann M, Helth A, Pilz S, Schmidt R, Calin M, Göttlicher M, Rohnke M, Janek J (2016) Oxidation treatments of beta-type Ti–40Nb for biomedical use. Surf Coat Technol 302:88–99. https://doi.org/10.1016/j.surfcoat.2016.05.036
221. Sedelnikova MB, Komarova EG, Sharkeev YP, Ugodchikova AV, Mushtovatova LS, Karpova MR, Sheikin VV, Litvinova LS, Khlusov IA (2019) Zn-, Cu- or Ag-incorporated micro-arc coatings on titanium alloys: properties and behavior in synthetic biological media. Surf Coat Technol 369:52–68. https://doi.org/10.1016/j.surfcoat.2019.04.021
222. Michalska J, Sowa M, Piotrowska M, Widziołek M, Tylko G, Dercz G, Socha RP, Osyczka AM, Simka W (2019) Incorporation of Ca ions into anodic oxide coatings on the Ti–13Nb–13Zr alloy by plasma electrolytic oxidation. Mater Sci Eng C 104:109957. https://doi.org/10.1016/j.msec.2019.109957
223. Tanase CE, Golozar M, Best SM, Brooks RA (2019) Cell response to plasma electrolytic oxidation surface-modified low-modulus β-type titanium alloys. Colloids Surf B 176:176–184. https://doi.org/10.1016/j.colsurfb.2018.12.064
224. Jang SH, Choe HC, Ko YM, Brantley WA (2009) Electrochemical characteristics of nanotubes formed on Ti–Nb alloys. Thin Solid Films 517:5038–5043. https://doi.org/10.1016/j.tsf.2009.03.166
225. Ossowska A, Sobieszczyk S, Supernak M, Zielinski A (2014) Morphology and properties of nanotubular oxide layer on the "Ti–13Zr–13Nb" alloy. Surf Coat Technol 258:1239–1248. https://doi.org/10.1016/j.surfcoat.2014.06.054
226. Hernández-López JM, Conde A, de Damborenea J, Arenas MA (2015) Correlation of the nanostructure of the anodic layers fabricated on Ti13Nb13Zr with the electrochemical impedance response. Corros Sci 94:61–69. https://doi.org/10.1016/j.corsci.2015.01.041
227. Kim HJ, Jeong YH, Choe HC, Brantley WA (2013) Surface morphology of TiN-coated nanotubular Ti–25Ta–xZr alloys for dental implants prepared by RF sputtering. Thin Solid Films 549:131–134. https://doi.org/10.1016/j.tsf.2013.09.045
228. Jeong YH, Choe HC, Brantley WA, Sohn IB (2013) Hydroxyapatite thin film coatings on nanotube-formed Ti–35Nb–10Zr alloys after femtosecond laser texturing. Surf Coat Technol 217:13–22. https://doi.org/10.1016/j.surfcoat.2012.11.066
229. Jeong YH, Choe HC, Brantley WA (2011) Nanostructured thin film formation on femtosecond laser-textured Ti–35Nb–xZr alloy for biomedical applications. Thin Solid Films 519:4668–4675. https://doi.org/10.1016/j.tsf.2011.01.014
230. Hieda J, Niinomi M, Nakai M, Cho K, Mohri T, Hanawa T (2014) Adhesive strength of medical polymer on anodic oxide nanostructures fabricated on biomedical β-type titanium alloy. Mater Sci Eng C 36:244–251. https://doi.org/10.1016/j.msec.2013.12.012
231. Li X, Chen T, Hu J, Li S, Zou Q, Li Y, Jiang N, Li H, Li J (2016) Modified surface morphology of a novel Ti–24Nb–4Zr–7.9Sn titanium alloy via anodic oxidation for enhanced interfacial biocompatibility and osseointegration. Colloids Surf B 144:265–275. https://doi.org/10.1016/j.colsurfb.2016.04.020
232. Hao YQ, Li SJ, Hao YL, Zhao YK, Ai HJ (2013) Effect of nanotube diameters on bioactivity of a multifunctional titanium alloy. Appl Surf Sci 268:44–51. https://doi.org/10.1016/j.apsusc.2012.11.142
233. Verissimo NC, Geilich BM, Oliveira HG, Caram R, Webster TJ (2015) Reducing *Staphylococcus aureus* growth on Ti alloy nanostructured surfaces through the addition of Sn. J Biomed Mater Res A 103:3757–3763. https://doi.org/10.1002/jbm.a.35517
234. Kim HJ, Jeong YH, Choe HC, Brantley WA (2014) Surface characteristics of hydroxyapatite coatings on nanotubular Ti–25Ta–xZr alloys prepared by electrochemical deposition. Surf Coat Technol 259:274–280. https://doi.org/10.1016/j.surfcoat.2014.03.013
235. Kim SH, Jeong YH, Choe HC, Brantley WA (2014) Morphology change of HA films on highly ordered nanotubular Ti–Nb–Hf alloys as a function of electrochemical deposition cycle. Surf Coat Technol 259:281–289. https://doi.org/10.1016/j.surfcoat.2014.03.006
236. Jeong YH, Kim EJ, Brantley WA, Choe HC (2014) Morphology of hydroxyapatite nanoparticles in coatings on nanotube-formed Ti–Nb–Zr alloys for dental implants. Vacuum 107:297–303. https://doi.org/10.1016/j.vacuum.2014.03.004
237. Byeon IS, Lee K, Choe HC, Brantley WA (2015) Surface morphology of Zn-containing hydroxyapatite (Zn–HA) deposited electrochemically on Ti–xNb alloys. Thin Solid Films 587:163–168. https://doi.org/10.1016/j.tsf.2015.01.028
238. Hussein MA, Kumar AM, Yilbas BS, Al-Aqeeli N (2017) Laser nitriding of the newly developed Ti–20Nb–13Zr at.% biomaterial alloy to enhance its mechanical and corrosion properties in simulated body fluid. J Mater Eng Perform 26:5553–5562. https://doi.org/10.1007/s11665-017-2955-5
239. Hussein MA, Yilbas B, Kumar AM, Drew R, Al-Aqeeli N (2018) Influence of laser nitriding on the surface and corrosion properties of Ti–20Nb–13Zr alloy in artificial saliva for dental applications. J Mater Eng Perform 27:4655–4664. https://doi.org/10.1007/s11665-018-3569-2
240. Zhao X, Zhang P, Wang X, Chen Y, Liu H, Chen L, Sheng Y, Li W (2018) In-situ formation of textured TiN coatings on biomedical titanium alloy by laser irradiation. J Mech Behav Biomed Mater 78:143–153. https://doi.org/10.1016/j.jmbbm.2017.11.019
241. Chan CW, Chang X, Bozorgzadeh MA, Smith GC, Lee S (2020) A single parameter approach to enhance the microstructural and mechanical properties of beta Ti–Nb alloy via open-air fiber

laser nitriding. Surf Coat Technol 383:125269. https://doi.org/10.1016/j.surfcoat.2019.125269
242. Geetha M, Mudali UK, Pandey ND, Asokamani R, Raj B (2004) Microstructural and corrosion evaluation of laser surface nitrided Ti–13Nb–13Zr alloy. Surf Eng 20:68–74. https://doi.org/10.1179/026708404225010595
243. Zhang T, Fan Q, Ma X, Wang W, Wang K, Shen P, Yang J (2019) Microstructure and mechanical properties of Ti–35Nb–2Ta–3Zr alloy by laser quenching. Front Mater 6:1–9. https://doi.org/10.3389/fmats.2019.00318
244. Mohseni H, Nandwana P, Tsoi A, Banerjee R, Scharf TW (2015) In situ nitrided titanium alloys: microstructural evolution during solidification and wear. Acta Mater 83:61–74. https://doi.org/10.1016/j.actamat.2014.09.026
245. Chan CW, Lee S, Smith G, Sarri G, Ng CH, Sharba A, Man HC (2016) Enhancement of wear and corrosion resistance of beta titanium alloy by laser gas alloying with nitrogen. Appl Surf Sci 367:80–90. https://doi.org/10.1016/j.apsusc.2016.01.091
246. Saud SN, Raheleh Hosseinian S, Bakhsheshi-Rad HR, Yaghoubidoust F, Iqbal N, Hamzah E, Ooi CHR (2016) Corrosion and bioactivity performance of graphene oxide coating on Ti–Nb shape memory alloys in simulated body fluid. Mater Sci Eng C 68:687–694. https://doi.org/10.1016/j.msec.2016.06.048
247. Lubov Donaghy C, McFadden R, Kelaini S, Carson L, Margariti A, Chan CW (2020) Creating an antibacterial surface on beta TNZT alloys for hip implant applications by laser nitriding. Opt Laser Technol 121:105793. https://doi.org/10.1016/j.optlastec.2019.105793
248. Donaghy CL, McFadden R, Smith GC, Kelaini S, Carson L, Malinov S, Margariti A, Chan CW (2019) Fibre laser treatment of beta TNZT titanium alloys for load-bearing implant applications: effects of surface physical and chemical features on mesenchymal stem cell response and *Staphylococcus aureus* bacterial attachment. Coatings. https://doi.org/10.3390/COATINGS9030186
249. González M, Salvagni E, Rodríguez-Cabello JC, Rupérez E, Gil FJ, Peña J, Manero JM (2013) A low elastic modulus Ti–Nb–Hf alloy bioactivated with an elastin-like protein-based polymer enhances osteoblast cell adhesion and spreading. J Biomed Mater Res A 101(A):819–826. https://doi.org/10.1002/jbm.a.34388
250. Hsu S-K, Ho W-F, Wu S-C, Chen Y-S, Hsu H-C (2016) In vitro study of Ti–Nb–Sn alloy surface modified with RGD peptide. Thin Solid Films 620:139–144. https://doi.org/10.1016/j.tsf.2016.09.063
251. Hieda J, Niinomi M, Nakai M, Kamura H, Tsutsumi H, Hanawa T (2012) Effect of terminal functional groups of silane layers on adhesive strength between biomedical Ti–29Nb–13Ta–4.6Zr alloy and segment polyurethanes. Surf Coat Technol 206:3137–3141. https://doi.org/10.1016/j.surfcoat.2011.12.044
252. Sun YS, Huang CY, Chen CS, Chang JH, Hou WT, Li SJ, Hao YL, Pan H, Huang HH (2018) Bone cell responses to a low elastic modulus titanium alloy surface immobilized with the natural cross-linker genipin. Surf Coat Technol 350:918–924. https://doi.org/10.1016/j.surfcoat.2018.03.069
253. Liu CF, Li SJ, Hou WT, Hao YL, Huang HH (2019) Enhancing corrosion resistance and biocompatibility of interconnected porous β-type Ti–24Nb–4Zr–8Sn alloy scaffold through alkaline treatment and type I collagen immobilization. Appl Surf Sci 476:325–334. https://doi.org/10.1016/j.apsusc.2019.01.084
254. Choe HC (2013) Photofunctionalization of EB-PVD HA-coated nano-pore surface of Ti–30Nb–xZr alloy for dental implants. Surf Coat Technol 228:S470–S476. https://doi.org/10.1016/j.surfcoat.2012.05.018
255. Nguyen PMH, Won DH, Kim BS, Jang YS, Nguyen TDT, Lee MH, Bae TS (2018) The effect of two-step surface modification for Ti–Ta–Mo–Zr alloys on bone regeneration: an evaluation using calvarial defect on rat model. Appl Surf Sci 442:630–639. https://doi.org/10.1016/j.apsusc.2018.02.211
256. Fojt J, Joska L, Hybasek V, Pruchova E, Malek J (2018) Impedance technique for monitoring of apatite precipitation from simulated body fluid. Electrochim Acta 271:158–164. https://doi.org/10.1016/j.electacta.2018.03.120
257. Rangel ALR, Falentin-Daudré C, da Silva Pimentel BNA, Vergani CE, Migonney V, Alves Claro APR (2020) Nanostructured titanium alloy surfaces for enhanced osteoblast response: a combination of morphology and chemistry. Surf Coat Technol 383:125226. https://doi.org/10.1016/j.surfcoat.2019.125226
258. Park SY, Jo CI, Choe HC, Brantley WA (2016) Hydroxyapatite deposition on micropore-formed Ti–Ta–Nb alloys by plasma electrolytic oxidation for dental applications. Surf Coat Technol 294:15–20. https://doi.org/10.1016/j.surfcoat.2016.03.056
259. Kazek-Kęsik A, Leśniak K, Orzechowska BU, Drab M, Wiśniewska A, Simka W (2018) Alkali treatment of anodized titanium alloys affects cytocompatibility. Metals (Basel). https://doi.org/10.3390/met8010029
260. Kazek-Kęsik A, Leśniak K, Zhidkov IS, Korotin DM, Kukharenko AI, Cholakh SO, Kalemba-Rec I, Suchanek K, Kurmaev EZ, Simka W (2017) Influence of alkali treatment on anodized titanium alloys in wollastonite suspension. Metals (Basel). https://doi.org/10.3390/met7090322
261. Kazek-Kęsik A, Nosol A, Płonka J, Śmiga-Matuszowicz M, Gołda-Cępa M, Krok-Borkowicz M, Brzychczy-Włoch M, Pamuła E, Simka W (2019) PLGA-amoxicillin-loaded layer formed on anodized Ti alloy as a hybrid material for dental implant applications. Mater Sci Eng C 94:998–1008. https://doi.org/10.1016/j.msec.2018.10.049
262. Wang X, Chen Y, Xu LJ, Xiao S, Kong F, Do Woo K (2011) Ti–Nb–Sn-hydroxyapatite composites synthesized by mechanical alloying and high frequency induction heated sintering. J Mech Behav Biomed Mater 4:2074–2080. https://doi.org/10.1016/j.jmbbm.2011.07.006
263. Majumdar P, Singh SB, Dhara S, Chakraborty M (2012) Influence of in situ TiB reinforcements and role of heat treatment on mechanical properties and biocompatibility of β Ti-alloys. J Mech Behav Biomed Mater 10:1–12. https://doi.org/10.1016/j.jmbbm.2012.02.014
264. Majumdar P, Singh SB, Dhara S, Chakraborty M (2015) Influence of boron addition to Ti–13Zr–13Nb alloy on MG63 osteoblast cell viability and protein adsorption. Mater Sci Eng C 46:62–68. https://doi.org/10.1016/j.msec.2014.10.012
265. Málek J, Hnilica F, Veselý J, Smola B, Březina V, Kolařík K (2014) The effect of boron addition on microstructure and mechanical properties of biomedical Ti35Nb6Ta alloy. Mater Charact 96:166–176. https://doi.org/10.1016/j.matchar.2014.07.015
266. Ou KL, Weng CC, Lin YH, Huang MS (2017) A promising of alloying modified beta-type titanium–niobium implant for biomedical applications: microstructural characteristics, in vitro biocompatibility and antibacterial performance. J Alloys Compd 697:231–238. https://doi.org/10.1016/j.jallcom.2016.12.120
267. Li YH, Shang XY (2020) Recent progress in porous TiNb-based alloys for biomedical implant applications. Mater Sci Technol (United Kingdom) 36:385–392. https://doi.org/10.1080/02670836.2020.1724415
268. Manoj A, Kasar AK, Menezes PL (2019) Tribocorrosion of porous titanium used in biomedical applications. J Bio Tribo Corros. https://doi.org/10.1007/s40735-018-0194-4
269. Li Y, Ding Y, Munir K, Lin J, Brandt M, Atrens A, Xiao Y, Kanwar JR, Wen C (2019) Novel β-Ti35Zr28Nb alloy scaffolds manufactured using selective laser melting for bone implant applications. Acta Biomater 87:273–284. https://doi.org/10.1016/j.actbio.2019.01.051

270. Zhuravleva K, Chivu A, Teresiak A, Scudino S, Calin M, Schultz L, Eckert J, Gebert A (2013) Porous low modulus Ti40Nb compacts with electrodeposited hydroxyapatite coating for biomedical applications. Mater Sci Eng C 33:2280–2287. https://doi.org/10.1016/j.msec.2013.01.049
271. Mutlu I, Yeniyol S, Oktay E (2016) Production and precipitation hardening of beta-type Ti–35Nb–10Cu alloy foam for implant applications. J Mater Eng Perform 25:1586–1593. https://doi.org/10.1007/s11665-016-1982-y
272. Soran MR, Mutlu I (2019) Production and anodising of highly porous Ti–Ta–Zr–Co alloy for biomedical implant applications. Corros Eng Sci Technol 54:54–61. https://doi.org/10.1080/1478422X.2018.1527820
273. Xu J, Zhang J, Bao L, Lai T, Luo J, Zheng Y (2018) Preparation and bioactive surface modification of the microwave sintered porous Ti–15Mo alloys for biomedical application. Sci China Mater 61:545–556. https://doi.org/10.1007/s40843-017-9098-2
274. Guo S, Meng Q, Zhao X, Wei Q, Xu H (2015) Design and fabrication of a metastable β-type titanium alloy with ultralow elastic modulus and high strength. Sci Rep 5:14688. https://doi.org/10.1038/srep14688
275. Zhang LC, Klemm D, Eckert J, Hao YL, Sercombe TB (2011) Manufacture by selective laser melting and mechanical behavior of a biomedical Ti–24Nb–4Zr–8Sn alloy. Scr Mater 65:21–24. https://doi.org/10.1016/j.scriptamat.2011.03.024
276. Li YH, Yang C, Wang F, Zhao HD, Qu SG, Li XQ, Zhang WW, Li YY (2015) Biomedical TiNbZrTaSi alloys designed by d-electron alloy design theory. Mater Des 85:7–13. https://doi.org/10.1016/j.matdes.2015.06.176
277. Liang SX, Feng XJ, Yin LX, Liu XY, Ma MZ, Liu RP (2016) Development of a new β-Ti alloy with low modulus and favorable plasticity for implant material. Mater Sci Eng C 61:338–343. https://doi.org/10.1016/j.msec.2015.12.076
278. Yang X, Hutchinson CR (2016) Corrosion-wear of β-Ti alloy alloy TMZF (Ti–12Mo–6Zr–2Fe) in simulated body fluid. Acta Biomater 42:429–439. https://doi.org/10.1016/j.actbio.2016.07.008
279. Lee YS, Niinomi M, Nakai M, Narita K, Cho K (2015) Predominant factor determining wear properties of β-type and (α+β)-type titanium alloys in metal-to-metal contact for biomedical applications. J Mech Behav Biomed Mater 41:208–220. https://doi.org/10.1016/j.jmbbm.2014.10.005
280. Lee Y, Niinomi M, Nakai M, Narita K, Cho K (2015) Differences in wear behaviors at sliding contacts for β-type and (α + β)-type titanium alloys in Ringer's solution and air. Mater Trans 56:317–326
281. Gongadze E, Kabaso D, Bauer S, Slivnik T, Schmuki P, van Rienen U, Iglič A (2011) Adhesion of osteoblasts to a nanorough titanium implant surface. Int J Nanomed. https://doi.org/10.2147/IJN.S21755
282. Xiong J, Wang X, Li Y, Hodgson PD (2011) Interfacial chemistry and adhesion between titanium dioxide nanotube layers and titanium substrates. J Phys Chem C 115:4768–4772. https://doi.org/10.1021/jp111651d
283. Yu D, Zhu X, Xu Z, Zhong X, Gui Q, Song Y, Zhang S, Chen X, Li D (2014) Facile method to enhance the adhesion of TiO_2 nanotube arrays to Ti substrate. ACS Appl Mater Interfaces 6:8001–8005. https://doi.org/10.1021/am5015716
284. Cao S, Huang W, Wu L, Tian M, Song Y (2018) On the interfacial adhesion between TiO_2 nanotube array layer and Ti substrate. Langmuir 34:13888–13896. https://doi.org/10.1021/acs.langmuir.8b03408
285. Li T, Gulati K, Wang N, Zhang Z, Ivanovski S (2018) Understanding and augmenting the stability of therapeutic nanotubes on anodized titanium implants. Mater Sci Eng C 88:182–195. https://doi.org/10.1016/j.msec.2018.03.007
286. Zhang Y, Han Y, Zhang L (2015) Interfacial structure of the firmly adhered TiO_2 nanotube films to titanium fabricated by a modified anodization. Thin Solid Films 583:151–157. https://doi.org/10.1016/j.tsf.2015.03.060
287. Fontes ACCA, Sopchenski L, Laurindo CAH, Torres RD, Popat KC, Soares P (2020) Annealing a effect on tribocorrosion and biocompatibility properties of TiO_2 nanotubes. J Bio Tribo Corros 6:1–12. https://doi.org/10.1007/s40735-020-00363-w
288. Alves SA, Rossi AL, Ribeiro AR, Toptan F, Pinto AM, Celis JP, Shokuhfar T, Rocha LA (2017) Tribo-electrochemical behavior of bio-functionalized TiO_2 nanotubes in artificial saliva: understanding of degradation mechanisms. Wear 384–385:28–42. https://doi.org/10.1016/j.wear.2017.05.005
289. Alves SA, Rossi AL, Ribeiro AR, Toptan F, Pinto AM, Shokuhfar T, Celis JP, Rocha LA (2018) Improved tribocorrosion performance of bio-functionalized TiO_2 nanotubes under two-cycle sliding actions in artificial saliva. J Mech Behav Biomed Mater 80:143–154. https://doi.org/10.1016/j.jmbbm.2018.01.038
290. Sun M, Yu D, Lu L, Ma W, Song Y, Zhu X (2015) Effective approach to strengthening TiO_2 nanotube arrays by using double or triple reinforcements. Appl Surf Sci 346:172–176. https://doi.org/10.1016/j.apsusc.2015.04.004
291. Ouyang HM, Fei GT, Zhang Y, Su H, Jin Z, Xu SH, De Zhang L (2013) Large scale free-standing open-ended TiO_2 nanotube arrays: stress-induced self-detachment and in situ pore opening. J Mater Chem C 1:7498–7506. https://doi.org/10.1039/c3tc31642d
292. Luz AR, De Souza GB, Lepienski CM, Kuromoto NK, Siqueira CJM (2018) Tribological properties of nanotubes grown on Ti–35Nb alloy by anodization. Thin Solid Films 660:529–537. https://doi.org/10.1016/j.tsf.2018.06.050
293. Mukherjee S, Dhara S, Saha P (2018) Laser surface remelting of Ti and its alloys for improving surface biocompatibility of orthopaedic implants. Mater Technol 33:106–118. https://doi.org/10.1080/10667857.2017.1390931
294. Shah A, Izman S, Ismail SNF, Mas Ayu H, Che Kob CG, Daud R, Abdul Kadir MR (2018) The influence of ultrasonic vibration frequency on the properties of TiN coated biomedical Ti–13Zr–13Nb. Metals (Basel) 8:1–10. https://doi.org/10.3390/met8050317
295. Wang P, Li H, Zhang Y, Liu H, Guo Y, Liu Z, Zhao S, Yin J, Guo Y (2014) Morphology of nanotube arrays grown on Ti–35Nb–2Ta–3Zr alloys with different deformations. Appl Surf Sci 290:308–312. https://doi.org/10.1016/j.apsusc.2013.11.073
296. Bahl S, Meka SRK, Suwas S, Chatterjee K (2018) Surface severe plastic deformation of an orthopedic Ti–Nb–Sn alloy induces unusual precipitate remodeling and supports stem cell osteogenesis through Akt signaling. ACS Biomater Sci Eng 4:3132–3142. https://doi.org/10.1021/acsbiomaterials.8b00406
297. Kheradmandfard M, Kashani-Bozorg SF, Kang KH, Penkov OV, Zarei Hanzaki A, Pyoun YS, Amanov A, Kim DE (2018) Simultaneous grain refinement and nanoscale spinodal decomposition of β phase in Ti–Nb–Ta–Zr alloy induced by ultrasonic mechanical impacts. J Alloys Compd 738:540–549. https://doi.org/10.1016/j.jallcom.2017.12.049
298. Zhang ZB, Hao YL, Li SJ, Yang R (2013) Fatigue behavior of ultrafine-grained Ti–24Nb–4Zr–8Sn multifunctional biomedical titanium alloy. Mater Sci Eng A 577:225–233. https://doi.org/10.1016/j.msea.2013.04.051
299. Gatina SA, Semenova IP, Ubyyvovk EV, Valiev RZ (2018) Phase transformations, strength, and modulus of elasticity of Ti–15Mo alloy obtained by high-pressure torsion. Inorg Mater Appl Res 9:14–20. https://doi.org/10.1134/S2075113318010136
300. Kolobov YR, Golosova OA, Manokhin SS (2018) Regularities of formation and degradation of the microstructure and properties of new ultrafine-grained low-modulus Ti–Nb–Mo–Zr alloys.

Russ J Non-Ferrous Met 59:393–402. https://doi.org/10.3103/S1067821218040090
301. Hee AC, Martin PJ, Bendavid A, Jamali SS, Zhao Y (2018) Tribo-corrosion performance of filtered-arc-deposited tantalum coatings on Ti–13Nb–13Zr alloy for bio-implants applications. Wear 400–401:31–42. https://doi.org/10.1016/j.wear.2017.12.017
302. Gnanavel S, Ponnusamy S, Mohan L (2018) Biocompatible response of hydroxyapatite coated on near-β titanium alloys by E-beam evaporation method. Biocatal Agric Biotechnol 15:364–369. https://doi.org/10.1016/j.bcab.2018.07.014
303. Anandan C, Mohan L (2013) In vitro corrosion behavior and apatite growth of oxygen plasma ion implanted titanium alloy β-21S. J Mater Eng Perform 22:3507–3516. https://doi.org/10.1007/s11665-013-0628-6
304. Guo L, Qin L, Kong F, Yi H, Tang B (2016) Improving tribological properties of Ti–5Zr–3Sn–5Mo–15Nb alloy by double glow plasma surface alloying. Appl Surf Sci 388:203–211. https://doi.org/10.1016/j.apsusc.2016.01.201
305. Yılmaz E, Gökçe A, Findik F, Gulsoy HO (2018) Metallurgical properties and biomimetic HA deposition performance of Ti–Nb PIM alloys. J Alloys Compd 746:301–313. https://doi.org/10.1016/j.jallcom.2018.02.274
306. Lauria I, Kutz TN, Böke F, Rütten S, Zander D, Fischer H (2019) Influence of nanoporous titanium niobium alloy surfaces produced via hydrogen peroxide oxidative etching on the osteogenic differentiation of human mesenchymal stromal cells. Mater Sci Eng C 98:635–648. https://doi.org/10.1016/j.msec.2019.01.023
307. Lario J, Amigó A, Segovia F, Amigó V (2018) Surface modification of Ti–35Nb–10Ta–15Fe by the double acid-etching process. Materials (Basel) 11:1–11. https://doi.org/10.3390/ma11040494
308. Mendes MWD, Ágreda CG, Bressiani AHA, Bressiani JC (2016) A new titanium based alloy Ti–27Nb–13Zr produced by powder metallurgy with biomimetic coating for use as a biomaterial. Mater Sci Eng C 63:671–677. https://doi.org/10.1016/j.msec.2016.03.052
309. Fajri H, Ariani W, Gunawarman, Tjong DH, Manjas M (2019) Corrosion behaviour of collagen coated and uncoated biomedical titanium alloy (TNTZ) within human synovial fluid. IOP Conf Ser Mater Sci Eng. https://doi.org/10.1088/1757-899X/547/1/012007
310. Arumugam MK, Hussein MA, Adesina AY, Al-Aqeeli N (2019) In vitro corrosion and bioactivity performance of surface-treated Ti–20Nb–13Zr alloys for orthopedic applications. Coatings 9:1–13. https://doi.org/10.3390/COATINGS9050344
311. Kasuga T, Mizuno T, Watanabe M, Nogami M, Niinomi M (2001) Calcium phosphate invert glass-ceramic coatings joined by self-development of compositionally gradient layers on a titanium alloy. Biomaterials 22:577–582. https://doi.org/10.1016/S0142-9612(00)00216-7
312. Dikici B, Niinomi M, Topuz M, Say Y, Aksakal B, Yilmazer H, Nakai M (2018) Synthesis and characterization of hydroxyapatite/TiO_2 coatings on the β-type titanium alloys with different sintering parameters using sol–gel method. Prot Met Phys Chem Surf 54:457–462. https://doi.org/10.1134/S2070205118030255
313. Dikici B, Niinomi M, Topuz M, Koc SG, Nakai M (2018) Synthesis of biphasic calcium phosphate (BCP) coatings on β-type titanium alloys reinforced with rutile-TiO_2 compounds: adhesion resistance and in-vitro corrosion. J Sol–Gel Sci Technol 87:713–724. https://doi.org/10.1007/s10971-018-4755-2
314. Kasuga T, Nogami M, Niinomi M, Hattori T (2003) Bioactive calcium phosphate invert glass-ceramic coating on β-type Ti–29Nb–13Ta–4.6Zr alloy. Biomaterials 24:283–290. https://doi.org/10.1016/S0142-9612(02)00316-2
315. dos Santos ML, dos Santos Riccardi C, de Almeida Filho E, Guastaldi AC (2018) Sol–gel based calcium phosphates coatings deposited on binary Ti–Mo alloys modified by laser beam irradiation for biomaterial/clinical applications. J Mater Sci Mater Med. https://doi.org/10.1007/s10856-018-6091-z
316. Gnanavel S, Ponnusamy S, Mohan L, Radhika R, Muthamizhchelvan C, Ramasubramanian K (2018) Electrochemical behavior of biomedical titanium alloys coated with diamond carbon in Hanks' solution. J Mater Eng Perform 27:1635–1641. https://doi.org/10.1007/s11665-018-3250-9
317. Gopal V, Chandran M, Rao MSR, Mischler S, Cao S, Manivasagam G (2017) Tribocorrosion and electrochemical behaviour of nanocrystalline diamond coated Ti based alloys for orthopaedic application. Tribol Int 106:88–100. https://doi.org/10.1016/j.triboint.2016.10.040
318. Travessa DN, da Silva Sobrinho AS, Júnior AMJ, Roche V (2019) Surface plasma nitriding of beta-titanium alloy bio-material. Key Eng Mater. https://doi.org/10.4028/www.scientific.net/KEM.813.328
319. Li H, Fu T, Li W, Alajmi Z, Sun J (2016) Hydrothermal growth of TiO_2-CaP nano-films on a Ti–Nb-based alloy in concentrated calcium phosphate solutions. J Nanopart Res 18:1–7. https://doi.org/10.1007/s11051-015-3315-8